Energy injection for mechanical systems through the method of Virtual Nonholonomic Constraints

by

Adan Moran-MacDonald

A thesis submitted in conformity with the requirements
for the degree of Master of Applied Science
Graduate Department of Electrical and Computer Engineering
University of Toronto

Abstract

Energy injection for mechanical systems through the method of Virtual Nonholonomic Constraints

Adan Moran-MacDonald
Master of Applied Science
Graduate Department of Electrical and Computer Engineering
University of Toronto
2020

TODO: Fill in the abstract

For Fry.

Acknowledgements

TODO: Fill in the acknowledgements

Contents

List of Symbols

Symbol	Definition
$\mathbf{n}$	The index set $\{1, \dots, n\}$ of natural numbers up to n.
$\mathbb{R}^n$	Real numbers in n dimensions.
$[\mathbb{R}]_T$	Real numbers modulo $T > 0$, with $[\mathbb{R}]_\infty = \mathbb{R}$.
$\mathbb{S}^1$	The unit circle, equivalent to $[\mathbb{R}]_{2\pi}$.
$\mathcal{Q}$	The configuration manifold of a system.
$C^r(X;Y)$	The space of r-times continuously differentiable functions from X to Y.
	If $r = \infty$, the space of smooth functions from X to Y.
$\mathbb{R}^{n \times m}$	The space of real-valued matrices with n rows and m columns.
I_n	The $n \times n$ identity matrix.
$\mathbf{0}_{n \times m}$	The $n \times m$ matrix of all zeros.
M_i	If M is a vector, the ith element of M.
	If M is a matrix, the ith column of M.
$M_{i,j}$	The value of row i, column j for the matrix M.
$\dot{x}$	Derivative of x with respect to time t.
$\nabla_v F$	If F is $\mathbb{R}$-valued, the gradient of F with respect to v.
	If F is $\mathbb{R}^{n \times n}$-valued and $v \in \mathbb{R}^m$, the block gradient $\left[\nabla_{v_1} F^\mathsf{T} \dots \nabla_{v_m} F^\mathsf{T}\right]^\mathsf{T} \in \mathbb{R}^{nm \times n}$.
dF_v	Total differential (Jacobian) of F, equivalent to $(\nabla_v F)^\mathsf{T}$.
$\operatorname{Hess} F$	If $F : \mathbb{R}^n \to \mathbb{R}$, the $n \times n$ Hessian matrix of double derivatives of F.
	If $F : \mathbb{R}^n \to \mathbb{R}^k$, the block matrix $(\operatorname{Hess} F_1, \dots, \operatorname{Hess} F_k) \in \mathbb{R}^{n \times nk}$.
$\partial_v \partial_w F$	Derivative matrix of $F : \mathbb{R}^n \times \mathbb{R}^m \to \mathbb{R}$, with (i,j) element $\frac{\partial^2 F}{\partial v_i \partial w_j}$.
$\delta_{i,j}$	The Kronecker delta: 1 if $i = j$ and 0 otherwise.
$\otimes$	The matrix kronecker product.
$\lVert\cdot\rVert$	The euclidean norm on $\mathbb{R}^n$.

TEST CITATIONS:

[1] [2] [3] [4] [5] [6] [7] [8] [9] [10] [11] [12] [13] [14] [15] [16] [17] [18] [19] [20] [21] [22] [23] [24] [25] [26] [27] [28] [29] [30] [31] [32] [33] [34] [35] [36] [37] [38] [39] [40] [41] [42] [43] [44] [45] [46] [47] [48] [49] [50] [51] [52] [53]

Chapter 1

Introduction

1.1 Literature Review

1.2 Statement of Contributions

1.3 Outline of the Thesis

1.4 Notation

Chapter 2

Development of Virtual Nonholonomic Constraints

2.1 Preliminaries on Analytical Mechanics

A mechanical system can be represented by N point masses where each point represents the center of mass of a physical body, along with r *equations of constraint* (EOC) which model the physical restrictions between these masses. The position of each point mass is described using three cartesian coordinates (one for each spatial axis), so the system as a whole can be described by a vector in $\mathbb{R}^{3N}$ with r EOC. The dynamics of the system are computed by deriving the $3N$ *equations of motion* (EOM) produced by Newton's second law $F = ma$. While this technique works for simple systems, it is tedius and becomes impossible to apply to complex mechanical systems where the forces are not explicitly known.

Rather than modeling a mechanical system by cartesian positions and constraints, it is often feasible to represent the position of the system using n independent scalar-valued variables $q_1, \ldots, q_n$ called *generalized coordinates*, where $n = 3N - r$ is the number of *degrees of freedom* (DOF) of the system [23]. For instance, Figure 2.1 shows a barbell on a $2D$-plane which can rotate freely on that plane. The barbell has $n = 3$ DOF, so it can be described by three independent generalized coordinates with no equations of constraint.

For the robotic systems of interest in this thesis, we assume that each generalized coordinate q_i represents either the distance or the angle between two parts of the system. Mathematically, each q_i takes values in $[\mathbb{R}]_{T_i}$, where $T_i = \infty$ if q_i represents a length or $T_i = 2\pi$ if q_i represents an angle. It is convention to collect the coordinates into a

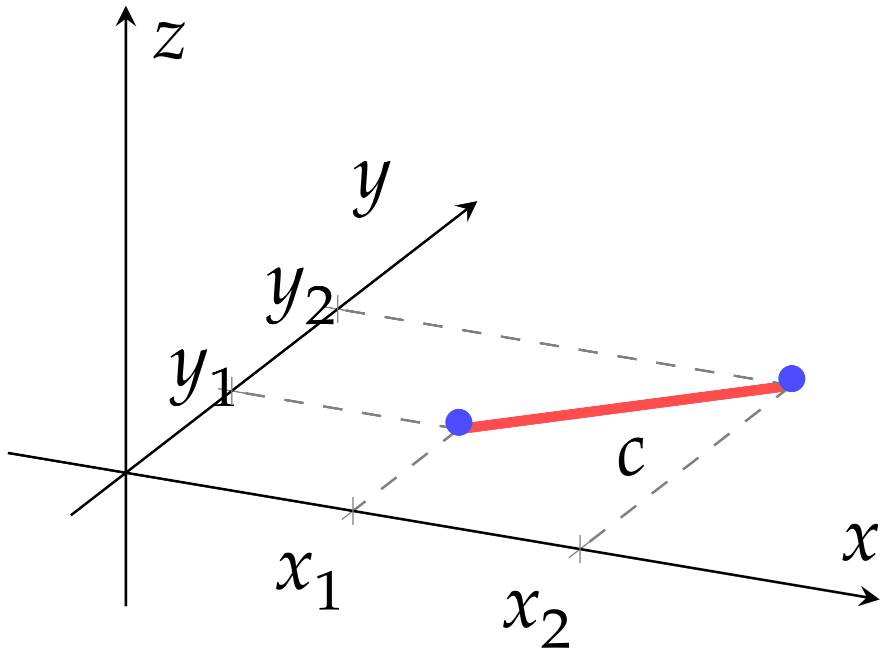

(A) The Newtonian representation of the barbell requires all six cartesian positions and the corresponding EOC.

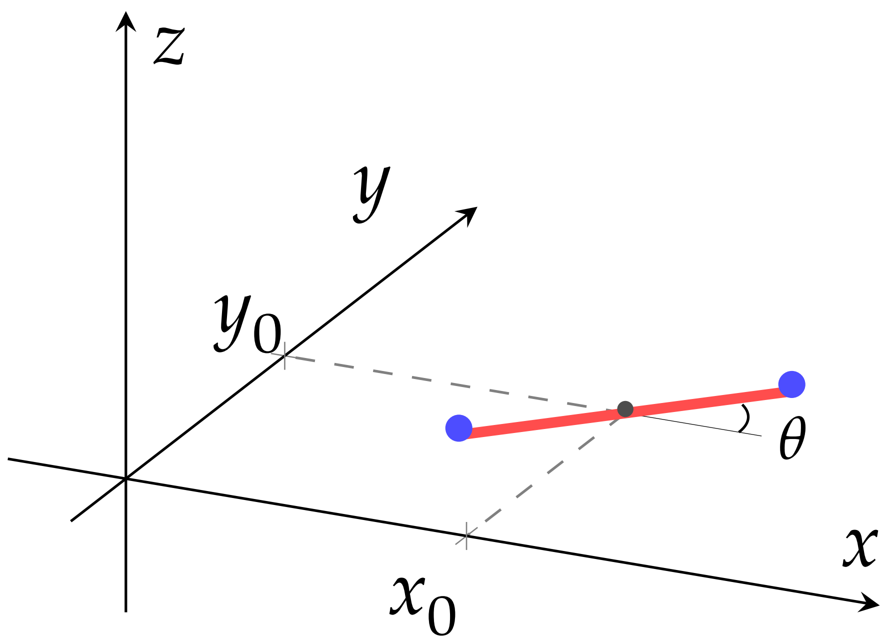

(B) One possible set of three generalized coordinates is (x_0, y_0, θ), which represent the position of the center of the bar and the angle of the barbell in the xy-plane.

FIGURE 2.1: A mechanical system with $N = 2$ point masses at $a = (x_1, y_1, z_1)$ and $b = (x_2, y_2, z_2)$, separated by a bar of length c. There are $r = 3$ EOC given by $\|a - b\| = c$, $z_1 = 0$, and $z_2 = 0$. This system has $n = 3$ degrees of freedom.

configuration $q = (q_1, \dots, q_n) \in \mathcal{Q}$ where the *configuration manifold* $\mathcal{Q}$ of the system is a so-called *generalized cylinder*

$$\mathcal{Q} = [\mathbb{R}]_{T_1} \times \cdot \times [\mathbb{R}]_{T_n}.$$

The derivative $\dot{q} = (\dot{q}_1, \dots, \dot{q}_n)$ of a configuration is called a *generalized velocity* of the system. For arbitrary systems, the space of allowable velocities depends on the current configuration of the system. However, since $\mathcal{Q}$ is a generalized cylinder, we find that $\dot{q} \in \mathbb{R}^n$. The combined vector $(q, \dot{q}) \in \mathcal{Q} \times \mathbb{R}^n$ is called a *state* of the system.

The field of analytical mechanics provides a computational method for finding the EOM of a system in generalized coordinates. The two most common analytical methods for modelling robotic systems are *Lagrangian* and *Hamiltonian* mechanics.

2.1.1 Lagrangian Mechanics

Lagrangian mechanics uses the kinetic energy $T(q, \dot{q})$ and potential energy $P(q)$ of the system to define the Lagrangian $\mathscr{L} : \mathcal{Q} \times \mathbb{R}^n \to \mathbb{R}$ defined by (2.1) [23],

$$\mathscr{L}(q, \dot{q}) = T(q, \dot{q}) - P(q). \tag{2.1}$$

When the mechanical system is actuated, the EOM are described by n second-order ordinary differential equations (ODEs) obtained from the *Euler-Lagrange equations* (2.2) with *generalized input forces* $\tau \in \mathbb{R}^k$

$$\frac{d}{dt}\left\{\frac{\partial \mathscr{L}}{\partial \dot{q}_i}\right\} - \frac{\partial \mathscr{L}}{\partial q_i} = B_i^\top(q)\tau. \tag{2.2}$$

The vector $B_i^\top : \mathcal{Q} \to \mathbb{R}^{1\times k}$ describes how the input forces shape the dynamics of q_i. The matrix $B : \mathcal{Q} \to \mathbb{R}^{n\times k}$ with

$$B(q) = \begin{bmatrix} - & B_1^\top(q) & - \\ & \vdots & \\ - & B_n^\top(q) & - \end{bmatrix},$$

is called the *input matrix* for the system. If $k < n$, we say the system is *underactuated* with degree of underactuation $(n - k)$.

Many actuated mechanical systems have quadratic kinetic energies, so that the Lagrangian can be written explicitly as

$$\mathscr{L}(q, \dot{q}) = \frac{1}{2}\dot{q}^\top D(q)\dot{q} - P(q), \tag{2.3}$$

where the *inertia matrix* $D : \mathcal{Q} \to \mathbb{R}^{n\times n}$ is a symmetric, positive definite matrix for all $q \in \mathcal{Q}$ and the potential function $P : \mathcal{Q} \to \mathbb{R}$ is smooth.

2.1.2 Hamiltonian Mechanics

Hamiltonian mechanics converts the n second-order ODEs generated by Lagrangian mechanics into an equivalent set of $2n$ first-order ODEs.

To do this, we first define the *conjugate of momentum p_i to q_i* by

$$p_i(q,\dot{q}) := \frac{\partial \mathcal{L}}{\partial \dot{q}_i}(q,\dot{q}). \tag{2.4}$$

To ease notation, we write $p = (p_1, \dots, p_n) \in \mathbb{R}^n$ and call p the *conjugate of momenta to* q. Note that each p_i is a linear function of $\dot{q}$, and one can typically solve for $\dot{q}(q,p)$ by inverting all the expressions from (2.4). The combined vector $(q,p) \in \mathcal{Q} \times \mathbb{R}^n$ is called a *phase* of the system.

The *Hamiltonian* of the system in (q,p) coordinates is the "Legendre transform" (2.5) of the Lagrangian [24],

$$\mathcal{H}(q,p) := p^\top \dot{q}(q,p) - \mathcal{L}(q,\dot{q}(q,p)). \tag{2.5}$$

The EOM in the Hamiltonian framework are the $2n$ first-order equations called *Hamilton's equations*. They are given by

$$\begin{cases} \dot{q} = \nabla_p \mathcal{H} \\ \dot{p} = -\nabla_q \mathcal{H} + B(q)\tau. \end{cases} \tag{2.6}$$

Here, $B(q) \in \mathbb{R}^{n\times k}$ is the same input matrix used by the Lagrangian framework, with $\tau \in \mathbb{R}^k$ the same vector of generalized input forces.

If the kinetic energy of the system is quadratic as in (2.3), the conjugate of momenta becomes $p = D(q)\dot{q}$. Since $D(q)$ is symmetric and positive definite, it is invertible at each $q \in \mathcal{Q}$. The Legendre transform (2.5) becomes

$$\begin{aligned} \mathcal{H}(q,p) &= p^\top D^{-1}(q)p - \left(\frac{1}{2}p^\top D^{-1}(q)p - P(q)\right) \\ &= \frac{1}{2}p^\top D^{-1}(q)p + P(q). \end{aligned}$$

Finding the derivative of each momentum coordinate yields

$$\dot{p}_i = -\frac{1}{2}p^\top \nabla_{q_i} D^{-1}(q)p - \frac{\partial P}{\partial q_i}(q) + B_i^\top(q)\tau.$$

Recall the Kronecker product of matrices [51], defined as follows.

Definition 2.1. Let $A \in \mathbb{R}^{n\times m}$ and $B \in \mathbb{R}^{r\times s}$. The Kronecker product $A \otimes B \in \mathbb{R}^{nr\times ms}$ is the matrix

$$A \otimes B = \begin{bmatrix} a_{1,1}B & \cdots & a_{1,m}B \\ \vdots & \ddots & \vdots \\ a_{n,1}B & \cdots & a_{n,m}B \end{bmatrix}.$$

Using the kronecker product, one can collect the derivative of momentum into the vector form

$$\dot{p} = -\frac{1}{2}(I_n \otimes p^\top)\nabla_q D^{-1}(q)p - \nabla_q P(q) + B(q)\tau.$$

In sum, when the kinetic energy is quadratic the Hamiltonian system reduces to

$$\mathscr{H}(q,p) = \frac{1}{2}p^\top D^{-1}(q)p + P(q), \tag{2.7}$$

$$\begin{cases} \dot{q} = D^{-1}(q)p \\ \dot{p} = -\frac{1}{2}(I_n \otimes p^\top)\nabla_q D^{-1}(q)p - \nabla_q P(q) + B(q)\tau. \end{cases} \tag{2.8}$$

Any set of coordinates (q,p) which satisfy Hamilton's equations under the Hamiltonian $\mathscr{H}$ are said to be *canonical coordinates* for the system. A change of coordinates $(q,p) \to (Q,P)$ is a *canonical transformation* if (Q,P) preserve the Hamiltonian structure; that is, if they are canonical coordinates under the Hamiltonian $\mathscr{H}\left(q(Q,P), p(Q,P)\right)$.

Landau and Lifschitz [24] provide a useful result for showing whether a given change of coordinates $(q,p) \to (Q,P)$ is a canonical transformation.

Definition 2.2. The *Poisson bracket* between the functions $f(q,p)$ and $g(q,p)$ is

$$[f,g] := \sum_{i=1}^{n} \frac{\partial f}{\partial p_i}\frac{\partial g}{\partial q_i} - \frac{\partial f}{\partial q_i}\frac{\partial g}{\partial p_i}. \tag{2.9}$$

Theorem 2.3. *A change of coordinates $(q,p) \to (Q,P)$ is a canonical transformation if and* *only if*

$$[Q_i, Q_j] = 0,$$
$$[P_i, P_j] = 0,$$
$$[P_i, Q_j] = \delta_{i,j},$$

for all $i, j \in \mathbf{n}$.

Proof. See (45.10) in [24]. □

Later in this chapter we will define a particular change of coordinates. The following Lemma allows us to prove it is a canonical transformation.

Lemma 2.4. *Let* $\mathscr{H}$ *be a Hamiltonian system in canonical coordinates* (q, p). *Let* $A \in \mathbb{R}^{n \times n}$ *be an orthogonal matrix. The change of coordinates* $(q, p) \to (Q = Aq, P = Ap)$ *is a canonical transformation.*

Proof. For any constant matrix A, the transformation $(Q = Aq, P = Ap)$ satisfies $\frac{\partial Q_i}{\partial p_m} = \frac{\partial P_i}{\partial q_m} = 0$ for all $i, m \in \mathbf{n}$. Hence,

$$[Q_i, Q_j] = \sum_{m=1}^{n} \frac{\partial Q_i}{\partial p_m}\frac{\partial Q_j}{\partial q_m} - \frac{\partial Q_i}{\partial q_m}\frac{\partial Q_j}{\partial p_m} = 0,$$
$$[P_i, P_j] = \sum_{m=1}^{n} \frac{\partial P_i}{\partial p_m}\frac{\partial P_j}{\partial q_m} - \frac{\partial P_i}{\partial q_m}\frac{\partial P_j}{\partial p_m} = 0.$$

Note that $(A_i)^\top (A^\top)_j = (A_i)^\top (A^{-1})_j = \delta_{i,j}$. Using this fact we see that the Poisson brackets between P_i and Q_j are given by

$$\begin{aligned}
[P_i, Q_j] &= \sum_{m=1}^{n} \frac{\partial P_i}{\partial p_m}\frac{\partial Q_j}{\partial q_m} - \frac{\partial P_i}{\partial q_m}\frac{\partial Q_j}{\partial p_m} \\
&= \sum_{m=1}^{n} A_{i,m}A_{j,m} - 0 \\
&= \sum_{m=1}^{n} A_{i,m}(A^\top)_{m,j} \\
&= (A_i)^\top (A^\top)_j \\
&= \delta_{i,j}.
\end{aligned}$$

Therefore, by Theorem 2.3, the coordinate change $(Q = Aq, P = Ap)$ is a canonical transformation. □

2.2 Simply Actuated Hamiltonian Systems

Suppose we are given a Hamiltonian mechanical system (2.7). Because τ is transformed by the input matrix $B(q)$ before entering the EOM, it is not in general clear how any particular input force τ_i will affect the dynamics of the system. In this section, we define a new class of Hamiltonian systems where the effect of the input forces is made obvious. This class of systems will form the backbone for the rest of the theory developed in this thesis.

Definition 2.5. Let $\mathscr{H}$ be an n-DOF Hamiltonian system with $k \leq n$ actuators. A set of canonical coordinates (q, p) for this system are said to be *simply actuated coordinates* if the input matrix $B(q) \in \mathbb{R}^{n \times k}$ is of the form

$$B(q) = \begin{bmatrix} \mathbf{0}_{(n-k)\times k} \\ I_k \end{bmatrix}.$$

The first $(n-k)$ coordinates, labelled q_u, are called the *unactuated coordinates*. The remaining k coordinates, labelled q_a, are called the *actuated coordinates*. When grouping them together, we will always put them in the order (q_u, q_a) to fit with the definition. The corresponding (p_u, p_a) are called the *unactuated* and *actuated momenta*, respectively.

Under the following assumptions on the input matrix, we will show that there is a canonical transformation of (2.7) into simply actuated coordinates.

Assumption 1. The input matrix $B(q) \equiv B \in \mathbb{R}^{n \times k}$ is constant, full rank, and $k < n$.

Assumption 2. There exists a matrix $B^\perp \in \mathbb{R}^{(n-k)\times n}$ which is right semi-orthogonal $\left(B^\perp (B^\perp)^\top = I_{(n-k)}\right)$ and which is a left-annihilator for B. That is, $B^\perp B = \mathbf{0}_{(n-k)\times k}$.

Assumption 2 requires the rows of $B^\perp$ to be unit vectors that are mutually orthogonal. In the case that $k = (n-1)$, the existence of any left annihilator $A^0 \in \mathbb{R}^{1\times n}$ implies the left annihilator $B^\perp := A^0/\|A^0\|$ will be a unit vector satisfying Assumption 2.

Lemma 2.6. *Suppose Assumption 1 holds. Then there exists a nonsingular matrix $\hat{T} \in \mathbb{R}^{k\times k}$ so that the regular feedback transformation*

$$\tau = \hat{T}\hat{\tau}$$

has a new input matrix $\hat{B}$ for $\hat{\tau}$ which is left semi-orthogonal. That is, $\hat{B}^\top \hat{B} = I_k$.

Proof. Since B is a constant matrix, it has a singular-value decomposition $B = U\Sigma V^\top$ where $U^{-1} = U^\top \in \mathbb{R}^{n\times n}$, $V^{-1} = V^\top \in \mathbb{R}^{k\times k}$, and $\Sigma \in \mathbb{R}^{n\times k}$ is defined by

$$\Sigma = \begin{bmatrix} \sigma_1 & 0 & \cdots & 0 \\ 0 & \sigma_2 & \cdots & 0 \\ \vdots & & \ddots & \vdots \\ 0 & 0 & \cdots & \sigma_k \\ - & & \mathbf{0}_{(n-k)\times k} & - \end{bmatrix},$$

where $\sigma_i \neq 0$ because B is full-rank [49]. Define $T \in \mathbb{R}^{k\times k}$ by

$$T = \begin{bmatrix} \frac{1}{\sigma_1} & 0 & \cdots & 0 \\ 0 & \frac{1}{\sigma_2} & \cdots & 0 \\ \vdots & & \ddots & \vdots \\ 0 & 0 & \cdots & \frac{1}{\sigma_k} \end{bmatrix}.$$

Letting $\hat{T} = VT$ and assigning the regular feedback transformation $\tau = \hat{T}\hat{\tau}$, we get a new input matrix for $\hat{\tau} \in \mathbb{R}^k$ given by

$$\hat{B} = B\hat{T} = BVT = U\begin{bmatrix} I_k \\ \mathbf{0}_{(n-k)\times k} \end{bmatrix},$$

which is still constant and full-rank. In particular, $\hat{B}^\top \hat{B} = T^\top \Sigma^\top \Sigma T = I_k$. □

In light of Lemma 2.6, there is no loss of generality by making the following assumption.

Assumption 3. Assume that the input matrix B is left semi-orthogonal, *i.e.*, $B^\top B = I_k$.

Let now $\mathbf{B} \in \mathbb{R}^{n\times n}$ be the following matrix:

$$\mathbf{B} = \begin{bmatrix} B^\perp \\ B^\top \end{bmatrix}.$$

Since $B^\perp$ is a left annihilator of B and both $B^\perp$ and $B^\top$ are right semi-orthogonal, it is easy to show that $\mathbf{B}$ is orthogonal.

Proof.

$$\mathbf{B}\mathbf{B}^\top = \begin{bmatrix} B^\perp (B^\perp)^\top & B^\perp B \\ (B^\perp B)^\top & B^\top B \end{bmatrix} = I_n.$$

Hence, $\mathbf{B}$ is invertible with $\mathbf{B}^{-1} = \mathbf{B}^\top$. $\square$

The following theorem shows that $\mathbf{B}$ provides a canonical transformation into simply actuated coordinates, so that only the actuated momenta are affected by the input forces.

Theorem 2.7. *Under Assumptions 1,2, and 3, the Hamiltonian system* (2.7) *has simply actuated canonical coordinates* $(Q = \mathbf{B}q, P = \mathbf{B}p)$. *The resulting dynamics are given by* (2.10),

$$\mathscr{H}(Q,P) = \frac{1}{2}P^\top M^{-1}(Q)P + V(Q), \tag{2.10}$$

$$\begin{cases} \dot{Q} = M^{-1}(Q)P \\ \dot{P} = -\frac{1}{2}(I_n \otimes P^\top)\nabla_Q M^{-1}(Q)P - \nabla_Q V(Q) + \begin{bmatrix} \mathbf{0}_{(n-k)\times k} \\ I_k \end{bmatrix}\tau, \end{cases}$$

where

$$\begin{aligned} M^{-1}(Q) &:= \mathbf{B}D^{-1}(\mathbf{B}^\top Q)\mathbf{B}^\top, \\ V(Q) &:= P(\mathbf{B}^\top Q). \end{aligned}$$

Proof. The change of coordinates $(Q = \mathbf{B}q, P = \mathbf{B}p)$ satisfies Lemma 2.4, making it a canonical transformation. Furthermore, since $\dot{P} = \mathbf{B}\dot{p}$, the new input matrix is given by

$$\mathbf{B}B = \begin{bmatrix} B^\perp B \\ B^\top B \end{bmatrix} = \begin{bmatrix} \mathbf{0}_{(n-k)\times k} \\ I_k \end{bmatrix},$$

which means $\big(Q = (q_u, q_a), P = (p_u, p_a)\big)$ are simply actuated coordinates for $\mathscr{H}$ as desired. $\square$

2.3 Virtual Nonholonomic Constraints

Let us imagine a child on a swing who wants to reach the largest height possible. To begin, the child pushes off the ground to imbue the swing with small oscillations. What allows them to increase the amplitude of these oscillations is the appropriate extension and retraction of their feet. If a roboticist were creating a machine to replicate this behaviour, they might design a robot whose legs extend and retract at specific time intervals. At first glance, this technique should work perfectly because the leg motion would synchronize with the swinging frequency, thereby injecting energy as quickly as is physically possible.

Unfortunately, a deeper analysis reveals the flaw with this design. Most children are not counting out the time in their head; rather, they observe their current position and velocity and adjust their legs as required. For example, many children have an adult pushing the swing, or perhaps they are swinging on a windy day. In either case, they adjust their leg motion accordingly when presented with these external disturbances, without keeping track of time. Hence, the standard control technique of tracking a function of time (known as *trajectory tracking*) does not truly replicate human behaviour. Even if the robot's legs perfectly track a specified trajectory, an external disturbance will desynchronize the leg motion with the swing - thereby stopping the amplitude-increasing effects.

Rather than tracking a trajectory over time, a more human-like behaviour is to force the robot's legs track a function of the swing's state. One recent control method known as *virtual holonomic constraints* (VHCs) uses the actuators to enforce a relation $h(q) = 0$ of the configuration [19]. This method has provided incredible results in the development of walking robots [27, 28], vehicle motion [30, 31], and has even been used to design a snake-like swimming robot [29].

The downside to VHCs is that they only depend on the configuration of a mechanical system, and not its generalized velocity. For the child on a swing, whether they extend or retract their legs depends on their direction of motion. This inherently requires knowledge of their current velocity, which precludes the usage of VHCs. A few authors have attempted to extend the theory of VHCs to enforce relations $h(q, \dot{q}) = 0$ of the full state to account for this drawback. Since these relations use actuators to restrict both the configuration and velocity of a system, they are called virtual *nonholonomic* constraints. This idea has been used for human-robot interaction [32–34], error-reduction on time-delayed systems [35], and has shown marked improvements to the field of bipedal locomotion [9, 36, 38]. Most interestingly, this nonholonomic approach is more robust than standard VHCs when applied to bipedal robotics [37]. In particular, virtual nonholonomic constraints may be capable of injecting and dissipating energy from a system in a robust manner, all while producing realistic biological motion. This is what we aim to prove in this thesis.

Unlike the theory of VHCs, there does not appear to be a standard definition of virtual nonholonomic constraints: all the applications listed above use their own definitions, which makes it difficult to compare and generalize their work.

This section will provide a standard characterization of virtual nonholonomic constraints using Hamiltonian mechanics. The goal is to provide a consistent, rigorous foundation for designing constraints on a general class of systems.

Definition 2.8. A *virtual nonholonomic constraint* (VNHC) *of order k* is a relation $h(q, p) = 0$ where $h : \mathcal{Q} \times \mathbb{R}^n \to \mathbb{R}^k$ is C^2, rank $\left(\left[dh_q, dh_p\right]\right) = k$ for all $(q, p) \in h^{-1}(0)$, and there exists a feedback controller $\tau(q, p)$ rendering the *constraint manifold* Γ invariant where

$$\Gamma = \left\{(q, p) \mid h(q, p) = 0, dh_q\dot{q} + dh_p\dot{p} = 0\right\}.$$

From the definition of VNHCs, one finds that the constraint manifold Γ is a $2(n-k)$-dimensional closed embedded submanifold of $\mathcal{Q} \times \mathbb{R}^n$. The next obvious question is the following: when does a feedback controller stabilizing Γ exist?

One approach to answering this question is to define the error term $e = h(q, p)$. If there exists some controller $\tau(q, p)$ driving $e \to 0$ and $\dot{e} \to 0$, then the same τ will necessarily stabilize Γ (under additional mild conditions, see [19]) [1].

We say that e is of *relative degree* $\{r_1, \dots, r_k\}$ if

1. Some component of τ appears at the r_i^{th} derivative of e_i for $i \in \{1, \dots, k\}$.

2. In the vector of time-derivatives $(e_1^{(r_1)}, \dots, e_k^{(r_k)})$, the vector τ is premultiplied by a nonsingular matrix.

With no further structure on $h(q, p)$, the control input τ usually appears after one derivative of e; unfortunately, if any e_i has relative degree $r_i = 1$ we may not be able to stabilize Γ. We could guarantee $e_i(t) \to 0$, but we could not in general guarantee $\dot{e}_i(t) \to 0$.

Requiring e to have relative degree $\{2, \dots, 2\}$ is much more useful, since it allows us to easily solve for a controller stabilizing Γ. This kind of relative degree requirement is already common in the VHC literature. Taking advantage of that precedent, we define a special type of VNHC that satisfies this property.

Definition 2.9. A VNHC $h(q, p) = 0$ of order k is *regular* if the output $e = h(q, p)$ is of relative degree $\{2, 2. \dots, 2\}$ everywhere on the constraint manifold Γ.

The authors of [9, 36, 37] observed that a relation which uses only the unactuated conjugate of momentum cannot have τ appearing after only one derivative. Of course, they performed their research in Lagrangian form; we will be using the Hamiltonian formulation from Chapter 2.2. As a reminder, our system is described in (q, p) coordinates

[1] The type of constraints we consider in this thesis are graphs of functions, and so meet these mild assumptions.

with $q = (q_u, q_a)$ and $p = (p_u, p_a)$ and has the dynamics

$$\mathscr{H}(q,p) = p^\top M^{-1}(q)p + V(q), \tag{2.11}$$

$$\begin{cases} \dot{q} = M^{-1}p \\ \dot{p} = -\frac{1}{2}(I_n \otimes p^\top)\nabla_q M^{-1}(q)p - \nabla_q V(q) + \begin{bmatrix} \mathbf{0}_{(n-k)\times k} \\ I_k \end{bmatrix} \tau. \end{cases} \tag{2.12}$$

Notation. We will write $q_u \in \mathcal{Q}_u$, $q_a \in \mathcal{Q}_a$ where $\mathcal{Q}_u \times \mathcal{Q}_a = \mathcal{Q}$. We also write $p_u \in \mathscr{P}_u := \mathbb{R}^{n-k}$ and $p_a \in \mathscr{P}_a := \mathbb{R}^k$, so that $p \in \mathscr{P} := \mathscr{P}_u \times \mathscr{P}_a = \mathbb{R}^n$. In this manner, the phase space of our system can be written as $\mathcal{Q} \times \mathscr{P}$.

Theorem 2.10. *A relation $h(q,p) = 0$ for system (2.11) is a regular VNHC of order k if and only if $dh_{p_a} = 0$ and*

$$\operatorname{rank}\left(\left(dh_q M^{-1}(q) - dh_{p_u}(I_{n-k} \otimes p^\top)\nabla_{q_u} M^{-1}(q) \right) \begin{bmatrix} \mathbf{0}_{(n-k)\times k} \\ I_k \end{bmatrix} \right) = k,$$

everywhere on the constraint manifold Γ.

Proof. Let $e = h(q,p) \in \mathbb{R}^k$. Then

$$\begin{aligned} \dot{e} &= dh_q \dot{q} + dh_p \dot{p} \\ &= dh_q M^{-1}(q)p + \\ &\begin{bmatrix} dh_{p_u} & dh_{p_a} \end{bmatrix} \left(-\frac{1}{2} \begin{bmatrix} (I_{n-k} \otimes p^\top)\nabla_{q_u} M^{-1}(q)p \\ (I_k \otimes p^\top)\nabla_{q_a} M^{-1}(q)p \end{bmatrix} - \begin{bmatrix} \nabla_{q_u} V(q) \\ \nabla_{q_a} V(q) \end{bmatrix} + \begin{bmatrix} \mathbf{0}_{(n-k)\times k} \\ I_k \end{bmatrix} \tau \right). \end{aligned}$$

If $dh_{p_a} \neq \mathbf{0}_{k\times k}$ for some (q,p) on Γ, then τ appears in $\dot{e}$ and the VNHC is not of relative degree $\{2, 2, \ldots, 2\}$. Hence, we must have that $dh_{p_a} = \mathbf{0}_{k\times k}$. Proceeding with this assumption, we now find that $h : \mathcal{Q} \times \mathscr{P}_u \to \mathbb{R}^k$, which means that

$$\dot{e} = dh_q M^{-1}(q)p - dh_{p_u}\left(\frac{1}{2}(I_{n-k} \otimes p^\top)\nabla_{q_u} M^{-1}(q)p + \nabla_{q_u} V(q) \right).$$

Taking one further derivative provides

$$\ddot{e} = \left(\frac{d}{dt}dh_q\right)M^{-1}(q)p + dh_q\left(\sum_{i=1}^{n}\frac{\partial M^{-1}}{\partial q_i}(q)\dot{q}_i\right)p + dh_qM^{-1}(q)\dot{p} - \left(\frac{d}{dt}dh_{p_u}\right)\left(\frac{1}{2}(I_{n-k}\otimes p^\top)\nabla_{q_u}M^{-1}(q)p + \nabla_{q_u}V(q)\right) - dh_{p_u}\left(\frac{1}{2}\frac{d}{dt}\left((I_{n-k}\otimes p^\top)\nabla_{q_u}M^{-1}(q)p\right) + \left(\frac{d}{dt}\nabla_{q_u}V(q)\right)\right).$$

Most of these terms do not involve $\dot{p}$ and hence do not contain τ, so we shorten this to

$$\ddot{e} = (\star) - dh_{p_u}\left(\frac{1}{2}\frac{d}{dt}\left((I_{n-k}\otimes p^\top)\nabla_{q_u}M^{-1}(q)p\right)\right) + dh_qM^{-1}(q)\begin{bmatrix}\mathbf{0}_{(n-k)\times k}\\ I_k\end{bmatrix}\tau.$$

Observe that the i^{th} row of $\frac{1}{2}\frac{d}{dt}\left((I_{n-k}\otimes p^\top)\nabla_{q_u}M^{-1}(q)p\right)$ is given by

$$\frac{1}{2}\frac{d}{dt}\left(p^\top\frac{\partial M^{-1}}{\partial q_{u_i}}(q)p\right) = p^\top\frac{\partial M^{-1}}{\partial q_{u_i}}(q)\dot{p} + \frac{1}{2}p^\top\left(\sum_{j=1}^{n}\frac{\partial^2 M^{-1}}{\partial q_{u_i}\partial q_j}\dot{q}_j\right)p.$$

Highlighting only the term containing τ, we get the vector form

$$\frac{1}{2}\frac{d}{dt}\left((I_{n-k}\otimes p^\top)\nabla_{q_u}M^{-1}(q)p\right) = (\star) + (I_{n-k}\otimes p^\top)\nabla_{q_u}M^{-1}(q)\begin{bmatrix}\mathbf{0}_{(n-k)\times k}\\ I_k\end{bmatrix}\tau.$$

Plugging this into $\ddot{e}$ reveals that

$$\ddot{e} = (\star) + \left(dh_qM^{-1}(q) - dh_{p_u}(I_{n-k}\otimes p^\top)\nabla_{q_u}M^{-1}(q)\right)\begin{bmatrix}\mathbf{0}_{(n-k)\times k}\\ I_k\end{bmatrix}\tau,$$

where $(\star)$ is a continuous function of q and p. For shorthand, we'll write

$$\ddot{e} = E(q,p) + H(q,p)\tau,$$

where E and H are defined appropriately. From the definition of regularity, the VNHC h is regular when e is of relative degree $\{2,\dots,2\}$, which is true if and only if the matrix premultiplying τ is nonsingular, and hence that H is invertible. This proves the theorem. □

Using the expression $\ddot{e} = E(q,p) + H(q,p)\tau$ from the proof of Theorem 2.10, a regular

VNHC of order k can be stabilized by[2] the output-linearizing phase-feedback controller

$$\tau(q,p) = -H^{-1}(q,p)\left(E(q,p) + k_p e + k_d \dot{e}\right), \tag{2.13}$$

where $k_p, k_d \in \mathbb{R}_{>0}$ are control parameters which can be tuned on the resulting linear system $\ddot{e} = -k_p e - k_d \dot{e}$.

Note that one generally cannot measure conjugate of momenta directly, as sensors on mechanical systems will only measure the state $(q, \dot{q})$. To implement this controller in practice, one must compute $p = M(q)\dot{q}$ at every iteration. In other words, this controller requires knowledge of the full state of the system.

Now that we have found a controller to enforce a regular VNHC of order k, we would like to determine the dynamics on the constraint manifold Γ. Intuitively, these dynamics should be parameterized by (q_u, p_u) since q_a is a function of these as specified by $h(q, p_u) = 0$. Unfortunately, $\dot{q}_u$ depends on p_a, and for general systems one cannot solve explicitly for p_a in terms of (q_u, p_u). This is because the $\dot{p}$ dynamics contains the coupling term $(I_n \otimes p^\top)\nabla_{q_u} M(q) p$.

We now introduce an assumption so we can solve explicitly for the constrained dynamics.

Assumption 4. The Hamiltonian system has an inertia matrix that does not depend on the unactuated coordinates:

$$\nabla_{q_u} M(q) = \mathbf{0}_{n(n-k)\times n}.$$

Theorem 2.11. *Let $\mathcal{H}$ be a mechanical system in simply actuated coordinates satisfying Assumption 4. Let $h(q, p_u) = 0$ be a regular VNHC of order k with constraint manifold Γ. Suppose that on Γ one can solve for q_a as a function $q_a = f(q_u, p_u)$. Then the constrained dynamics are given by*

$$\left.\begin{aligned} \dot{q}_u &= \begin{bmatrix} I_{(n-k)} & \mathbf{0}_{(n-k)\times k} \end{bmatrix} M^{-1}(q) p \\ \dot{p}_u &= -\nabla_{q_u} V(q) \end{aligned}\right|_{\substack{q_a = f(q_u, p_u) \\ p_a = g(q_u, p_u)}}, \tag{2.14}$$

where

$$g(q_u, p_u) := \left(dh_q M^{-1}(q) \begin{bmatrix} \mathbf{0}_{(n-k)\times k} \\ I_k \end{bmatrix}\right)^{-1} \left(dh_{p_u} \nabla_{q_u} V(q) - dh_q M^{-1}(q) \begin{bmatrix} I_{n-k} \\ \mathbf{0}_{k\times(n-k)} \end{bmatrix} p_u\right)\Bigg|_{q_a = f(q_u, p_u)}. \tag{2.15}$$

[2]Under additional mild conditions [19]

Proof. Setting $e = h(q, p_u)$ and using the fact that $\nabla_{q_u} M^{-1}(q) = 0$, we find that

$$\dot{e} = dh_q M^{-1}(q)p - dh_{p_u} \nabla_{q_u} V(q).$$

Observe that

$$\begin{aligned} dh_q M^{-1}(q)p &= dh_q M^{-1}(q) \begin{bmatrix} p_u \\ p_a \end{bmatrix} \\ &= dh_q M^{-1}(q) \begin{bmatrix} I_{n-k} & \mathbf{0}_{(n-k)\times k} \\ \mathbf{0}_{k\times(n-k)} & I_k \end{bmatrix} \begin{bmatrix} p_u \\ p_a \end{bmatrix} \\ &= dh_q M^{-1}(q) \begin{bmatrix} I_{n-k} \\ \mathbf{0}_{k\times(n-k)} \end{bmatrix} p_u + dh_q M^{-1}(q) \begin{bmatrix} \mathbf{0}_{(n-k)\times k} \\ I_k \end{bmatrix} p_a. \end{aligned}$$

On the constraint manifold, we have $e = \dot{e} = 0$, which means

$$dh_q M^{-1}(q) \begin{bmatrix} \mathbf{0}_{(n-k)\times k} \\ I_k \end{bmatrix} p_a = dh_{p_u} \nabla_{q_u} V(q) - dh_q M^{-1}(q) \begin{bmatrix} I_{n-k} \\ \mathbf{0}_{k\times(n-k)} \end{bmatrix} p_u.$$

Since h is regular and $\nabla_{q_u} M^{-1}(q) = 0$, we have that

$$\operatorname{rank}\left(dh_q M^{-1}(q) \begin{bmatrix} \mathbf{0}_{(n-k)\times k} \\ I_k \end{bmatrix} \right) = k.$$

Solving for p_a gives

$$p_a(q, p_u) = \left(dh_q M^{-1}(q) \begin{bmatrix} \mathbf{0}_{(n-k)\times k} \\ I_k \end{bmatrix} \right)^{-1} \left(dh_{p_u} \nabla_{q_u} V(q) - dh_q M^{-1}(q) \begin{bmatrix} I_{n-k} \\ \mathbf{0}_{k\times(n-k)} \end{bmatrix} p_u \right).$$

This yields a function $p_a(q, p_u)$. However, on Γ we have $q_a = f(q_u, p_u)$, which we use to solve for $p_a = g(q_u, p_u)$. Since q_a and p_a can be computed directly from (q_u, p_u), the dynamics on Γ are parameterized only by $(\dot{q}_u, \dot{p}_u)$. □

Theorem 2.11 shows that, for a particular class of systems and constraints, the dynamics on Γ are entirely described by the $2(n-k)$ unactuated coordinates. This is true regardless of the number of degrees of freedom of the system.

The following corollay applies Theorem 2.11 to systems with only one unactuated coordinate.

Corollary. *Let $\mathcal{H}$ be the system* (2.10) *with degree of underactuation one. Suppose $\mathcal{H}$ satisfies*

Assumption 4. Let $h(q, p_u) = 0$ *be a regular VNHC of order* $(n-1)$ *of the form* $h(q, p_u) = q_a - f(q_u, p_u)$*, where* f *is a suitably defined* C^2 *function. Then* $dh_q = \begin{bmatrix} -\partial_{q_u} f & I_{(n-1)} \end{bmatrix}$*. Defining* $e_1 := (1, 0, \dots, 0) \in \mathbb{R}^n$*, the actuated momentum is*

$$p_a = -\left(dh_q M^{-1}(q) \begin{bmatrix} \mathbf{0}_{1\times(n-1)} \\ I_{(n-1)} \end{bmatrix} \right)^{-1} \left(\partial_{p_u} f \partial_{q_u} V + dh_q M^{-1}(q) e_1 p_u \right) \Bigg|_{q_a = f(q_u, p_u)} . \tag{2.16}$$

Since $q_u \in [\mathbb{R}]_{T_u}$ *for some* $T_u \in]0, \infty]$ *and* $p_u \in \mathbb{R}$*, the orbit* $(q_u(t), p_u(t))$ *traces out a curve on the 2D constraint manifold* $\Gamma = [\mathbb{R}]_{T_u} \times \mathbb{R}$ *which we call the* (q_u, p_u)*-plane.*

We conclude this chapter by formalizing the notion of energy injection for VNHCs. To glean some intuition for this idea, suppose our mechanical system satisfies the above corollary so that the constraint manifold Γ is the (q_u, p_u)-plane. If any initial condition of the constrained dynamics converges to the origin, the system must be losing energy because the unactuated momentum p_u is decreasing. Any notion of energy injection must therefore require that the origin of Γ repels all solutions. Furthermore, periodic solutions prevent the system from attaining higher speeds, so the constrained dynamics should not have closed orbits or limit cycles. Finally, we want the unactuated momentum to increase on average, regardless of its initial value. This intuition is generalized to ODEs on manifolds by the following definition.

Definition 2.12. Let $M = [\mathbb{R}]_{T_1} \times \cdots \times [\mathbb{R}]_{T_n}$ (where $T_1, \dots, T_n \in \{2\pi, \infty\}$) be an n-dimensional generalized cylinder. Let $f : M \to \mathbb{R}^n$ be smooth with $f(0) = 0$ and let $D \subset M$ be open. The system described by $\dot{x} = f(x)$ *gains energy on* D if these conditions are satisfied:

1. If $0 \in D$, then 0 is a repeller (or equivalently, it is asymptotically stable in negative time).

2. For all compact sets $K \subset D$ and for almost every initial condition $x(0) \in K$, there exists $T > 0$ such that $x(t) \notin K$ $(\forall t > T)$.

The system *loses energy on* D if it gains energy in negative-time.

The second property of Definition 2.12 allows the system to have unstable equilibria, but not limit cycles nor closed orbits. The next definition ties this notion of energy gain to VNHCs.

Definition 2.13. A regular VNHC $h(q, p) = 0$ with constraint manifold Γ *injects (dissipates) energy on* $D \subset \Gamma$ if the constrained dynamics gain (lose) energy everywhere on D, except possibly on a set of measure zero.

2.4 Summary of Results

In this chapter, we developed the framework of virtual nonholonomic constraints for underactuated Hamiltonian mechanical systems. We made the following assumptions:

1. The input matrix $B(q) \equiv B \in \mathbb{R}^{n\times k}$ is constant and full rank.
2. The input matrix has a left-annihilator $B^\perp \in \mathbb{R}^{(n-k)\times n}$.
3. The annihilator matrix $B^\perp$ is right semi-orthogonal.

These assumptions allowed us to define a canonical change of coordinates into the simply actuated coordinates $(q, p) \in \mathcal{Q} \times \mathcal{P}$, where $q = (q_u, q_a)$ and $p = (p_u, p_a)$.

We defined a virtual nonholonomic constraint as a function $h \in C^2(\mathcal{Q} \times \mathcal{P}; \mathbb{R}^k)$ which has no singular points on its constraint manifold

$$\Gamma = \left\{(q, p) \mid h(q, p) = 0, dh_q\dot{q} + dh_p\dot{p} = 0\right\}.$$

We then showed that a VNHC $h : \mathcal{Q} \times \mathcal{P}_u \to \mathbb{R}^k$ is regular if and only if the square matrix

$$\left(dh_q M^{-1}(q) - dh_{p_u}(I_{n-k} \otimes p^\top)\nabla_{q_u} M^{-1}(q)\right)\begin{bmatrix}\mathbf{0}_{(n-k)\times k}\\ I_k\end{bmatrix}$$

is invertible on Γ.

To find the explicit equations for constrained dynamics of a regular VNHC, we made the following assumptions:

- The inertia matrix satisfies $\nabla_{q_u} M(q) = \mathbf{0}_{n(n-k)\times n}$.
- On Γ, one can solve for q_a as a function of (q_u, p_u).

If these assumptions hold, one can solve for $p_a = g(q_u, p_u)$ on Γ. The constrained dynamics are then given by $(\dot{q_u}, \dot{p_u})$ subject to $h(q, p_u) = 0$ and $p_a = g(q_u, p_u)$.

Finally, we saw the benefit of using VNHCs is that they reduce the dimensionality of the system from $2n$ equations of motion to $2(n-k)$ equations, which significantly reduces the complexity of analyzing large systems. In particular, if the system has degree of underactuation one, the dynamics reduce to a 2D system on the "(q, p)-plane" $[\mathbb{R}]_T \times \mathbb{R}$.

Chapter 3

Application of VNHCS: The Variable Length Pendulum

3.1 Motivation

The variable length pendulum (VLP) is a classical underactuated dynamical system which is often used to model the motion of a person on a swing [8, 16]. The VLP also represents the motion of the load at the end of a crane, the (simplified) motion of a gymnast on a bar [15], and the tuned-mass-damper systems which stabilize skyscrapers [41].

The motion of the VLP has been well studied (see for instance [39]), and many control mechanisms exist to stabilize trajectories of the system. While many of these controllers are time-dependent, Xin and Liu [20] offer a time-independent technique to inject energy into the VLP. They design a controller through a technique called *energy shaping* and prove that it stabilizes any desired energy level set. However, their control input depends on a pre-specified target energy and requires knowledge of the current total energy of the VLP. This makes their energy injection mechanism "ad-hoc" in the sense that it is tailored very specifically to the VLP, and is not generalizable to a larger methodology.

It may be better to base the control design on natural biological behaviour. In this chapter we will make use of the general VNHC framework developed in Chapter 2 to add and remove energy from the VLP in a time-independent manner. We'll show that, unlike energy shaping, VNHCs can be used to stabilize energy levels while maintaining the structured motion of a human on a swing.

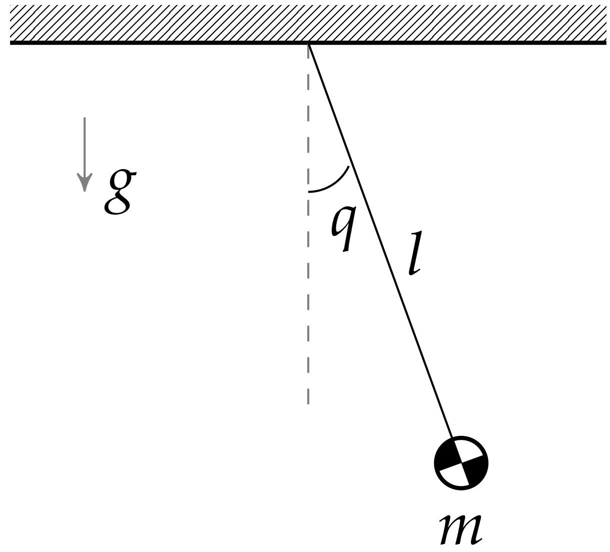

FIGURE 3.1: The variable length pendulum is a mass attached to the tip of a massless rod which can change length.

3.2 Dynamics of the Variable Length Pendulum

We will model the VLP as a point mass m connected to a fixed pivot by a massless rod of varying length l with angle $q \in \mathbb{S}^1$ from the vertical, as in Figure 3.1. We will ignore any damping and frictional forces in this model. In a realistic VLP, the rod length l varies between some minimum length $\underline{l} \geq 0$ and some maximum length $\bar{l} > \underline{l}$. The configuration of the VLP is the vector $\mathbf{q} := (q, l) \in \mathbb{S}^1 \times [\underline{l}, \bar{l}]$.

Using this configuration, we will compute the Hamiltonian dynamics of the system. The Cartesian position of the mass at the tip of the pendulum is given by $x = (l\sin(q), -l\cos(q))$, while its velocity is $\dot{x} = (\dot{l}\sin(q) + l\cos(q)\dot{q}, -\dot{l}\cos(q) + l\sin(q)\dot{q})$. Computing the kinetic energy T yields

$$T(\mathbf{q}, \dot{\mathbf{q}}) = \frac{1}{2}m\|\dot{x}\|^2 = \frac{1}{2}m\left(\dot{l}^2 + l^2\dot{q}^2\right).$$

The potential energy P with respect to the pivot (under a gravitational acceleration g) is

$$P(\mathbf{q}) = -mgl\cos(q).$$

Collecting the kinetic energy into a quadratic form, we get the Lagrangian

$$\mathscr{L}(\mathbf{q}, \dot{\mathbf{q}}) = \frac{1}{2}\dot{\mathbf{q}}^\top D(\mathbf{q})\dot{\mathbf{q}} - P(\mathbf{q}) = \frac{1}{2}\begin{bmatrix}\dot{q} & \dot{l}\end{bmatrix}\begin{bmatrix}ml^2 & 0 \\ 0 & m\end{bmatrix}\begin{bmatrix}\dot{q} \\ \dot{l}\end{bmatrix} + mgl\cos(q).$$

Computing the conjugate of momenta to $\mathbf{q}$, we get

$$\mathbf{p} := \begin{bmatrix} p \\ p_l \end{bmatrix} = \begin{bmatrix} ml^2\dot{q} \\ m\dot{l} \end{bmatrix}.$$

Performing the Legendre transform on $\mathscr{L}$ and setting $M(\mathbf{q}) := D(\mathbf{q})$, $V(\mathbf{q}) := P(\mathbf{q})$, we get the Hamiltonian (2.11) whose dynamics (2.12) resolve to

$$\mathscr{H} = \frac{1}{2}\begin{bmatrix} p & p_l \end{bmatrix}\begin{bmatrix} \frac{1}{ml^2} & 0 \\ 0 & \frac{1}{m} \end{bmatrix}\begin{bmatrix} p \\ p_l \end{bmatrix} - mgl\cos(q), \tag{3.1}$$

$$\begin{cases} \dot{q} = \frac{p}{ml^2} \\ \dot{l} = \frac{p_l}{m} \\ \dot{p} = -mgl\sin(q) \\ \dot{p}_l = \frac{p^2}{ml^3} + mg\cos(q) + \tau. \end{cases}$$

The control input is a force $\tau \in \mathbb{R}$ affecting the dynamics of p_l, acting collinearly with the rod. We assume the force does not affect the dynamics of p in any way - that is, the control input cannot enact any lateral force on the pendulum. This makes the VLP into an underactuated mechanical system with degree of underactuation one. It is also a useful assumption because it means $(\mathbf{q}, \mathbf{p})$ are simply actuated coordinates, which allows us to apply the theory of VNHCs we developed in Chapter 2.

Let us define the VNHC $l = L(q, p)$, by which we mean we are actually defining the VNHC $h(\mathbf{q}, \mathbf{p}) = l - L(q, p) = 0$ of order 1. The VLP satisfies $\nabla_q M^{-1}(\mathbf{q}) = \mathbf{0}_{2\times 2}$. By Theorem 2.10, $h(\mathbf{q}, \mathbf{p})$ is a regular VNHC whenever $L(q, p)$ is C^2 because

$$dh_{\mathbf{q}} M^{-1}(\mathbf{q})B = \begin{bmatrix} -\frac{\partial L}{\partial q} & 1 \end{bmatrix}\begin{bmatrix} \frac{1}{ml^2} & 0 \\ 0 & \frac{1}{m} \end{bmatrix}\begin{bmatrix} 0 \\ 1 \end{bmatrix} = \frac{1}{m}$$

is always full rank. The constraint manifold is $\Gamma = \mathbb{S}^1 \times \mathbb{R}$, which is parameterized by the unactuated phase (q, p). By Theorem 2.11, the constrained dynamics are described entirely by $(\dot{q}, \dot{p})$ with l replaced by $L(q, p)$:

$$\begin{cases} \dot{q} = \frac{p}{mL^2} \\ \dot{p} = -mgL\sin(q). \end{cases} \tag{3.2}$$

Note that we suppress the function notation of $L(q, p)$ for clarity.

The total mechanical energy of the system restricted to the constraint manifold is

(A) A person standing on a swing has their center of mass close to the pivot.

(B) When a person squats on a swing, their center of mass extends away from the pivot.

FIGURE 3.2: The VLP representation of a person on a standing swing.

given by (3.3), where $L(q,p)$ and $\dot{L}(q,p)$ are known.

$$E(q,p) = \frac{1}{2}\frac{p^2}{mL^2} + \frac{1}{2}\dot{L}^2 - mgL\cos(q). \tag{3.3}$$

In the rest of this chapter, we will derive a C^2 function $L(q,p)$ based on natural human motion. This function will produce constrained dynamics that inject energy into the VLP.

3.3 The VLP Constraint

To motivate why a VNHC could inject energy into the VLP in a human-like manner, we will examine a person standing on a swing. As can be seen in Figure 3.2, a person's center of mass moves closer to the swing's pivot when they stand, and moves away from the pivot when they squat. This is equivalent to the VLP model from Figure 3.1, where standing and squatting correspond to shortening and lengthening the pendulum respectively.

The action of regulating pendulum length to inject energy into the VLP is known as "pumping". Piccoli and Kulkarni [16] asked whether the pumping strategy performed by children is time-optimal, assuming the children could squat or stand instantaneously.

Indeed, they discovered that children increase the height of their swing as fast as is physically possible.

A child's optimal pumping strategy is the following: they stand at the lowest point of the swing, and squat at the highest point. Looking at the VLP representation, the pendulum shortens at the bottom of the swing, and lengthens at the top. For an intuitive explanation, conservation of angular momentum indicates that shortening the pendulum at the bottom forces the mass to gain speed to compensate for the reduced length [8]. Energy is not conserved in this process, so the pendulum gains kinetic energy and reaches a higher point at the peak of its swing. Lengthening the pendulum when it reaches this peak means gravity imparts a larger angular momentum to the mass by the time it reaches the bottom of its swing, which in turn is converted to a higher velocity when the pendulum is shortened. By alternating these processes, the pendulum experiences an average net gain in rotational energy.

Notice that the child's pumping strategy requires knowledge of when the system is at the "bottom" or "top" of the swing. Since being at the bottom is equivalent to having angle $q = 0$ and being at the top is equivalent to having momentum $p = 0$, a controller based on this strategy will necessarily involve the full unactuated phase (q, p). This is why we must use VNHCs instead of other methods (such as VHCs) to perform this maneuver.

The time-optimal controller from [16] is, in our notation,

$$L^\star(q, p) := -\operatorname{sgn}(qp),$$

which is a piecewise-continuous controller that varies between ± 1. We could set our constraint to be $l = L^\star(q, p)$, but this is not a VNHC because it is not C^2. Additionally, it would force us to assume that $l \in \{-1, 0, 1\}$ and that one can switch l instantaneously. Since we need to enforce the constraint using the physical input τ (which would ideally emulate realistic human motion), we cannot use $L^\star$ as our VNHC. We will instead find an alternate representation of $L^\star$ which can be converted into a VNHC, and which allows $l \in [\underline{l}, \bar{l}]$.

Figure 3.3a displays $L^\star(q, p)$ on the (q, p)-plane. Note that the length remains constant inside each quadrant and changes only when it crosses one of the axes. Using this fact, we can redefine the time-optimal pumping strategy as a function of $\theta := \arctan_2(p, q)$. Abusing notation, we denote this by $L^\star(\theta)$, which is defined in (3.4). Figure 3.3b shows

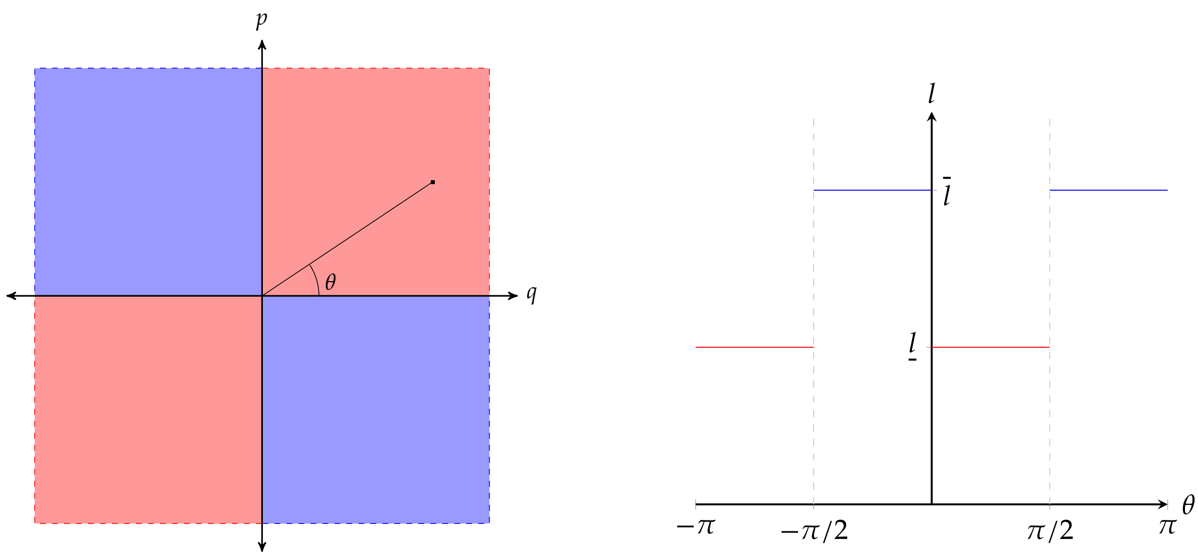

(A) The time-optimal controller $L^\star(q,p)$ mapped onto the (q,p)-plane. Here, red corresponds to $L^\star(q,p) = -1$ and blue to $L^\star(q,p) = 1$.

(B) The time-optimal controller converted to the alternate representation $L^\star(\theta)$.

Figure 3.3: The time-optimal controller for a standing swing as derived by [16]. The colour red corresponds to standing, blue to squatting, and $\theta := \operatorname{arctan}_2(p,q)$ is the angle of the VLP phase in the (q,p)-plane.

the graph of $L^\star(\theta)$, where now the length varies between $[\underline{l}, \bar{l}]$ rather than $\{-1,0,1\}$.

$$L^\star(\theta) := \begin{cases} \bar{l} & \theta \in [-\frac{\pi}{2}, 0[\cup [\frac{\pi}{2}, \pi[\\ \underline{l} & \theta \in [-pi, -\frac{\pi}{2}[\cup [0, \frac{\pi}{2}[. \end{cases} \tag{3.4}$$

We now define a continuous function which approximates $L^\star(\theta)$. Let $\Delta l := (\bar{l} - \underline{l})/2$ and $l_{\text{avg}} := (\bar{l} + \underline{l})/2$. Let $T \in]0, \frac{\pi}{2}]$ be a parameter of our choosing. By intelligently attaching sinusoids of frequency $\omega = \frac{\pi}{T}$ to $L^\star(\theta)$ (see Figure 3.4), we get a family of C^1 constraints $L_T(\theta)$ parameterized by T:

$$L_T(\theta) := \begin{cases} \bar{l} & \theta \in \left[-\frac{\pi}{2} + \frac{T}{2}, -\frac{T}{2}\right] \cup \left[\frac{\pi}{2} + \frac{T}{2}, \pi - \frac{T}{2}\right] \\ \underline{l} & \theta \in \left[-\pi + \frac{T}{2}, -\frac{\pi}{2} - \frac{T}{2}\right] \cup \left[\frac{T}{2}, \frac{\pi}{2} - \frac{T}{2}\right] \\ -\Delta l \sin(\omega(\theta + \pi)) + l_{\text{avg}} & \theta \in \left[-\pi, -\pi + \frac{T}{2}\right] \\ -\Delta l \sin(\omega\theta) + l_{\text{avg}} & \theta \in [-\frac{T}{2}, \frac{T}{2}] \\ \Delta l \sin(\omega(\theta - a)) + l_{\text{avg}} & \theta \in \left[a - \frac{T}{2}, a + \frac{T}{2}\right] \text{ for } a \in \left\{-\frac{\pi}{2}, \frac{\pi}{2}\right\} \\ -\Delta l \sin(\omega(\theta - \pi)) & \theta \in \left[\pi - \frac{T}{2}, \pi\right]. \end{cases} \tag{3.5}$$

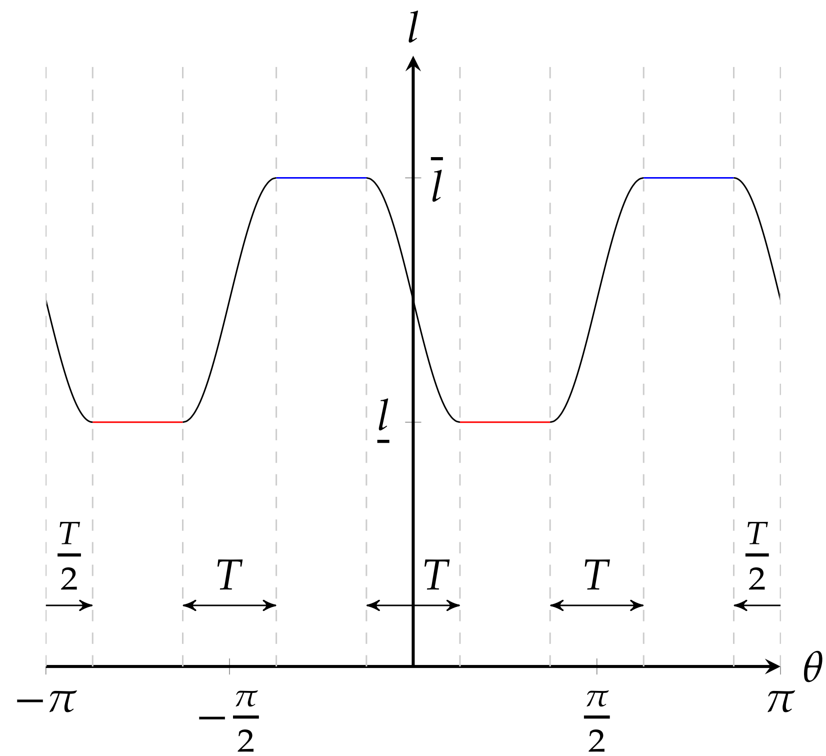

Figure 3.4: The continuous VLP constraint $l = L_T(\theta)$.

This family of constraints approximates $L^\star(\theta)$ because

$$\lim_{T \to 0} L_T(\theta) = L^\star(\theta).$$

Unfortunately, while $L_T(\theta)$ is continuously-differentiable, it is not twice-differentiable for most values of T. If we wish to use it as a VNHC, we must ensure that either the generalized forces τ acting on p_l can be discontinuous (which is certainly achievable by humans), or we must find a value of T where this constraint is at least C^2. Thankfully, setting $T = \frac{\pi}{2}$ yields the smooth function $L_{\frac{\pi}{2}}(\theta)$, which can be simplified from (3.5) into

$$L_{\frac{\pi}{2}}(\theta) = -\Delta l \sin(2\theta) + l_{\text{avg}}. \tag{3.6}$$

This smooth constraint is plotted for demonstration in Figure 3.5.

Because $L_{\frac{\pi}{2}}(\theta)$ is smooth and it approximates $L^\star(\theta)$, we set our VNHC to be

$$h(\mathbf{q}, \mathbf{p}) = l - L_{\frac{\pi}{2}}\left(\theta(q, p)\right).$$

We can now prove our VNHC injects energy into the VLP. As part of the proof, we will require the following lemma.

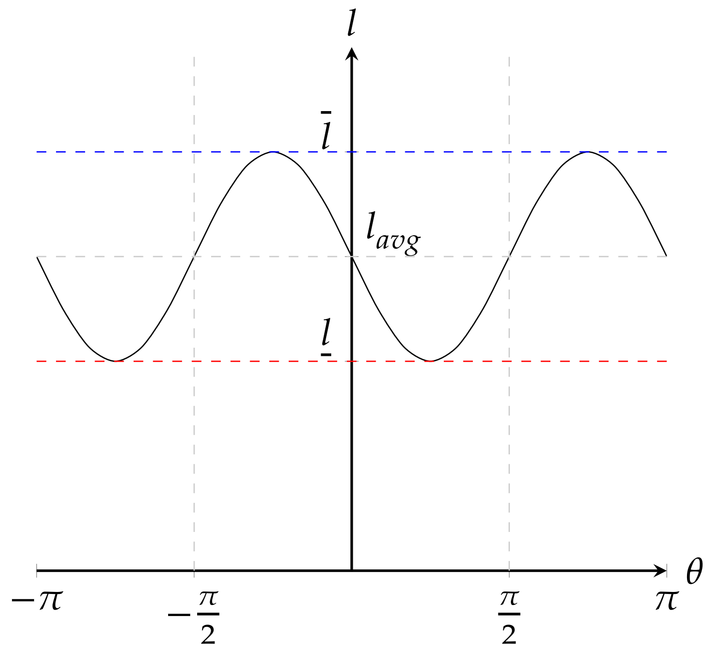

FIGURE 3.5: The smoothed VLP constraint $l = L_{\frac{\pi}{2}}(\theta)$.

Lemma 3.1. *For any $x, y \in \mathbb{R}$,*

$$\operatorname{sgn}\left(x^3 - y^3\right) = \operatorname{sgn}\left(x - y\right).$$

Proof. Observe that $x^3 - y^3 = (x-y)(x^2 + xy + y^2)$. The inequality $x^2 + xy + y^2 \geq 0$ holds because

$$x^2 + xy + y^2 = \left(x + \frac{y}{2}\right)^2 + \frac{3y^2}{4} \geq 0,$$

which proves the lemma. □

We will show that the constrained dynamics trace out a curve on the (q, p)-plane which is diverging from the origin. This implies that the momentum p is increasing in magnitude whenever the curve hits the p-axis, which in turn means the VLP is gaining energy on average.

Theorem 3.2. *Define $\theta := \text{arctan}_2(p, q)$. Let $L : \mathbb{S}^1 \to [\underline{l}, \bar{l}]$ be a C^2 function of θ. A regular VNHC of the form $h(\mathbf{q}, \mathbf{p}) = l - L(\theta)$ for the VLP injects energy on the constraint manifold $\Gamma = \mathbb{S}^1 \times \mathbb{R}$ if there exists $l_{avg} \in [\underline{l}, \bar{l}]$ such that*

$$\left(l_{avg} - L(\theta)\right) sin(2\theta) \geq 0 \; \forall \theta \in \mathbb{S}^1, \tag{3.7}$$

with the property that the inequality is strict except at $\theta \in \{0, \frac{\pi}{2}, \pi, \frac{3\pi}{2}\}$*. If instead*

$$\left(l_{avg} - L(\theta)\right) sin(2\theta) \leq 0 \ \forall \theta \in \mathbb{S}^1,$$

the VNHC dissipates energy on Γ.

Proof. We will first show that, under the given assumptions, the origin of the constrained dynamics (3.2) is a repeller, and for that we consider the negative time system obtained from (3.2) by reversing the sign of the vector field:

$$\begin{cases} \dot{q} = -\frac{p}{mL^2} \\ \dot{p} = mgL\sin(q). \end{cases} \tag{3.8}$$

The state space of (3.8) is $\mathbb{S}^1 \times \mathbb{R}$, and the system has two equilibria, $(q, p) = (0, 0)$ and $(q, p) = (\pi, 0)$. We need to show that the equilibrium $(q, p) = (0, 0)$ is asymptotically stable for (3.8).

Consider the Lyapunov function candidate

$$E_{\text{avg}}(q, p) := \frac{1}{2}\frac{p^2}{ml_{\text{avg}}^2} + mgl_{\text{avg}}(1 - \cos(q)),$$

which corresponds to the energy of VLP when the pendulum length is fixed at l_{avg}. The function E_{avg} is positive definite at $(0, 0)$, and has compact sublevel sets on $\mathbb{S}^1 \times \mathbb{R}$. The derivative of E_{avg} along (3.8) is

$$\dot{E}_{\text{avg}} = \frac{g\sin(q)p\left(L(\theta)^3 - l_{\text{avg}}^3\right)}{l_{\text{avg}}^2 L(\theta)^2}. \tag{3.9}$$

It is easy to show that

$$\text{sgn}\left(\sin(q)p\right) = \text{sgn}\left(\sin(2\theta)\right).$$

Furthermore, by Lemma 3.1 we have

$$\text{sgn}\left(L(\theta)^3 - l_{\text{avg}}^3\right) = \text{sgn}\left(L(\theta) - l_{\text{avg}}\right),$$

and therefore,

$$\begin{aligned}\operatorname{sgn}\left(\dot{E}_{\text{avg}}\right) &= \operatorname{sgn}\left(\sin(q)p\left(L(\theta)^3 - l_{\text{avg}}^3\right)\right) \\ &= \operatorname{sgn}\left(\sin(2\theta)\left(L(\theta) - l_{\text{avg}}\right)\right) \\ &= -\operatorname{sgn}\left((l_{\text{avg}} - L(\theta))\sin(2\theta)\right) \\ &\leq 0 \text{ (by assumption).} \end{aligned} \tag{3.10}$$

We have thus shown that $\dot{E}_{\text{avg}} \leq 0$, and therefore the equilibrium $(q,p) = (0,0)$ is stable for (3.8). We now apply the Krasovskii-LaSalle invariance principle, and consider the largest subset of $Z = \left\{(q,p) \in \mathbb{S}^1 \times \mathbb{R} \mid \dot{E}_{\text{avg}}(q,p) = 0\right\}$. We see from (3.9) that $\dot{E}_{\text{avg}}(q,p)$ is zero when $p = 0$, $\sin(q) = 0$, or $L(\theta) = l_{\text{avg}}$. This latter condition by assumption is met when $\theta \in \{0, \pi/2, \pi, 3\pi/2\}$, or equivalently when either $q = 0$ or $p = 0$. All in all, we have that

$$Z = \left\{(q,p) \in \mathbb{S}^1 \times \mathbb{R} \mid q = 0\right\} \cup \left\{(q,p) \in \mathbb{S}^1 \times \mathbb{R} \mid p = 0\right\}.$$

It is easily seen that the largest invariant subset of Z is the union of the two equilibria

$$\Omega = \{(0,0)\} \cup \{(\pi,0)\}.$$

Since all sublevel sets of E_{avg} are compact, the Krasovskii-LaSalle invariance principle implies that the set Ω is globally attractive [50]. Since the two equilibria are isolated, and since $(q,p) = (0,0)$ is stable, we deduce that the equilibrium $(q,p) = (0,0)$ is asymptotically stable for the negative time system (3.8), and thus it is a repeller for the constrained dynamics in (3.2).

We now prove that almost all solutions of the reduced dynamics (3.2) escape compact sets in finite time, *i.e.*, that for each compact subset K of $\mathbb{S}^1 \times \mathbb{R}$, and for almost every condition $(q_0, p_0) \in K$, there exists $T > 0$ such that $(q(t), p(t)) \notin K$ for all $t > T$, where $(q(t), p(t))$ denotes the solution of (3.2) with $(q(0), p(0)) = (q_0, p_0)$. In what follows, we denote by $x = (q,p)$ the state of the reduced dynamics (3.2). Also, we denote by Π^- the stable manifold of the equilibrium $(\pi, 0)$ for system (3.2), defined as

$$\Pi^- := \left\{x(0) \in \mathbb{S}^1 \times \mathbb{R} \mid \lim_{t\to\infty} x(t) = (\pi,0)\right\}.$$

The linearization of system (3.2) at the equilibrium $(\pi, 0)$ has a system matrix given by

$$\begin{bmatrix} 0 & -\frac{1}{mL(0)^2} \\ -mgL(0) & 0 \end{bmatrix}, \tag{3.11}$$

whose spectrum is $\{\pm\sqrt{g/L(0)}\}$. Since one eigenvalue of (3.11) is positive and one is negative, the stable manifold theorem implies that the stable manifold Π^- is a one-dimensional immersed submanifold of $\mathbb{S}^1 \times \mathbb{R}$, and thus is a set of measure zero [53].

Let $K \subset \mathbb{S}^1 \times \mathbb{R}$ be an arbitrary compact set and let $x(0) \in K \setminus (\Pi^- \cup \{(0,0)\})$. Since $x(0) \notin \Pi^-$, we have that

$$x(t) \nrightarrow_{t\to\infty} (\pi, 0). \tag{3.12}$$

Suppose, by way of contradiction, that for each $T > 0$ there exists $t' > T$ such that $x(t') \in K$. Letting

$$k := \max_{x\in K} E_{\text{avg}}(x),$$

and $E_k = \{x \mid E_{\text{avg}}(x) \leq k\}$, we have that $K \subset E_k$, and thus $x(t') \in E_k$. We have shown earlier that the function E_{avg} is nonincreasing along solutions of (3.8), which implies that $E_{\text{avg}}(x(t))$ is nondecreasing for solutions of the reduced dynamics (3.2), and therefore the half orbit $x([0,t'])$ is contained fully within E_k. In particular, $x(T) \in E_k$. Since this is true for each $T > 0$, we deduce that $x(t) \in E_k$ for all $t \in [0, \infty[$. Since E_k is compact, $x(t)$ has a positive limit set in E_k which, by the Poincaré-Bendixson theorem, is either an equilibrium or a closed orbit [52]. We will show this positive limit set must be an equilibrium and thereby reach a contradiction.

In order to rule out closed orbits, suppose that the reduced dynamics (3.2) have a periodic solution $z(t)$. Since $E_{\text{avg}}(z(t))$ is nondecreasing and $z(t)$ is periodic, it must be that $E_{\text{avg}}(z(t))$ is constant, or $\dot{E}_{\text{avg}}(z(t)) \equiv 0$. We have shown earlier that[1]

$$\{x \mid \dot{E}_{\text{avg}}(x) = 0\} = \{(q,p) \mid q = 0\} \cup \{(q,p) \mid p = 0\},$$

and the only invariant subset of this set is the union of two disjoint equilibria. Since the orbit $z(\mathbb{R})$ is an invariant set which is connected, $z(\mathbb{R})$ must be an equilibrium and cannot be a nontrivial closed orbit.

Returning to the Poincarè-Bendixson theorem, the positive limit set of $x(t)$ must be an equilibrium and, by (3.12), this equilibrium must be $(0,0)$. Since we have chosen $x(0) \neq (0,0)$, and since $(q,p) = (0,0)$ is a repeller, $x(t)$ cannot converge to $(0,0)$, which gives a contradiction.

We conclude that the VNHC injects energy into the VLP on $\mathbb{S}^1 \times \mathbb{R}$. By flipping the inequality of (3.7) we find the VLP is gaining energy in negative-time, so the VNHC is dissipating energy. $\square$

[1] We have shown it for the negative time system (3.8), but changing the sign of the vector field does not change the set where $\dot{E}_{\text{avg}} = 0$ nor the invariant sets.

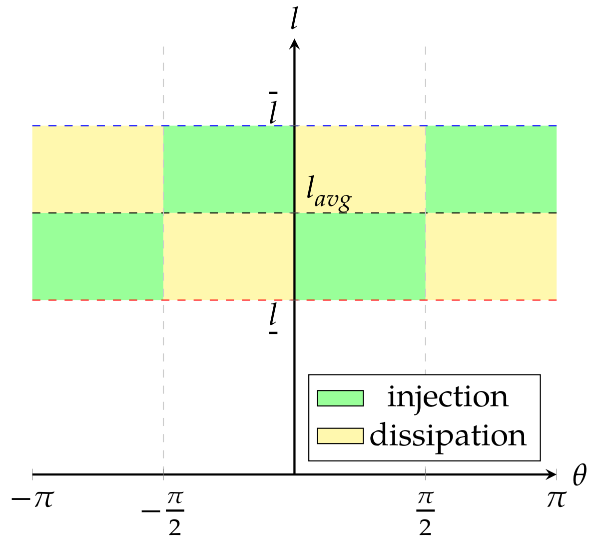

FIGURE 3.6: Any VNHC of the form $l = L(\theta)$ where $L(\theta)$ is entirely contained within the green (yellow) regions will inject (dissipate) energy.

Corollary. *Recall that*

$$L_{\frac{\pi}{2}}(\theta) := -\Delta l \sin(2\theta) + l_{avg},$$

and define

$$L^{-}_{\frac{\pi}{2}}(\theta) := \Delta l \sin(2\theta) + l_{avg}.$$

The VNHC $l = L_{\frac{\pi}{2}}(\theta)$ injects energy into the VLP, while $l = L^{-}_{\frac{\pi}{2}}(\theta)$ dissipates energy.

Proof. Both VNHCs satisfy Theorem 3.2 because

$$\left(l_{\text{avg}} - L_{\frac{\pi}{2}}(\theta)\right)\sin(2\theta) = \Delta l \sin^2(2\theta) \geq 0,$$

and

$$\left(l_{\text{avg}} - L^{-}_{\frac{\pi}{2}}(\theta)\right)\sin(2\theta) = -\Delta l \sin^2(2\theta) \leq 0,$$

where the inequalities are strict everywhere except the coordinate axes. □

The class of VNHCs which satisfies Theorem 3.2 is illustrated graphically in Figure 3.6. To stabilize specific energy level sets, one simple approach is to switch between injection and dissipation VNHCs when the momentum p reaches a pre-determined value at the bottom of the swing. For the VNHCs we designed in this chapter, this means toggling between $L_{\frac{\pi}{2}}(\theta)$ and $L^{-}_{\frac{\pi}{2}}(\theta)$, with some hysteresis to avoid infinite switching.

Theorem 3.2 provides an alternate explanation for why the optimal pumping strategy $L^{\star}(\theta)$ works so well at injecting energy: it maximizes the derivative of E_{avg} under the restriction $l \in [\underline{l}, \bar{l}]$, so that the orbit in the (q, p)-plane diverges from the origin as fast as possible.

Let us define $(L^\star)^-(\theta)$ by swapping the order of $\underline{l}$ and $\bar{l}$ in $L^\star(\theta)$:

$$(L^\star)^-(\theta) := \begin{cases} \underline{l} & \theta \in [-\frac{\pi}{2}, 0[\cup [\frac{\pi}{2}, \pi[\\ \bar{l} & \theta \in [-pi, -\frac{\pi}{2}[\cup [0, \frac{\pi}{2}[. \end{cases}$$

Since this function *minimizes* the derivative of E_{avg} under the restriction $l \in [\underline{l}, \bar{l}]$, one might predict that $(L^\star)^-(\theta)$ is the optimal energy dissipation strategy for the VLP. This is, in fact, true. Piccoli and Kulkarni [16] showed that squatting at the lowest point of a swing and standing at the highest (instead of standing and squatting, respectively) produces the time-optimal trajectory for *stopping* a standing swing.

All together, the theory developed in this chapter shows that VNHCs can replicate the time-optimal pumping/dissipation strategies performed by humans on swings. Furthermore, we see that VNHCs are a powerful tool for creating simple energy stabilization techniques based on natural human motion.

3.4 Simulation Results

Chapter 4

Application of VNHCs: The Acrobot

4.1 Motivation

The acrobot is a two-link pendulum, actuated at the center joint (as in Figure 4.1). Since its first description in 1990 [43], the acrobot has become a benchmark problem in control theory; it is an underactuated mechanical system which produces complex nonlinear motion from an easy-to-describe model. The acrobot models a gymnast on a bar, since it represents a torso (top link) and legs (bottom link) with motion generated by the swinging of the legs at the hips. It is also one of the simplest models for a biped walking robot [44].

Controlling the acrobot is a nontrivial task because it is not feedback linearizable [43]. Several researchers have studied the swing-up problem of driving the acrobot to its equilibrium point above the bar using partial feedback linearization [45], energy-based control [17, 46], and through studying human motion [18, 47].

In gymnastics terminology, a “giant” is the motion a gymnast performs to achieve full rotations around the bar [48]. We are interested in using VNHCs to generate giant motion, with the aim of stabilizing desired energy levels. The control of giant motion for the acrobot has been studied in [5, 18], and some authors have used virtual holonomic constraints to achieve this behaviour [2, 3, 21]. However, these controllers are neither intuitive nor easy to design: [2] defines a constraint by inverting a trajectory in time onto the state space; [3] requires a cascade controller to stabilize both a constraint and a desired limit cycle in the state space; and [21] enforces the giant by adding an extra state to estimate velocity, which increases the dimensionality of the problem in a crude approach to using VNHCs.

In this chapter we will design a physically-intuitive VNHC which generates giant motion and prove the acrobot gains energy. In the process of completing this proof,

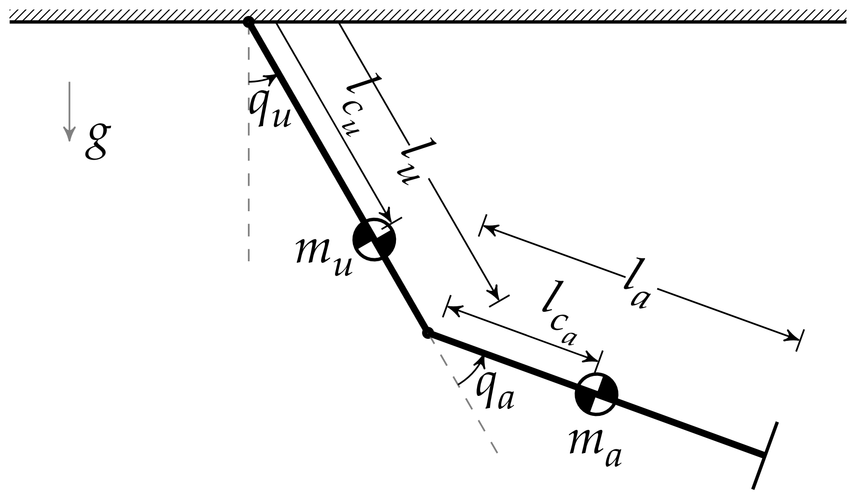

Figure 4.1: The general acrobot model, represented by two weighted rods differing in both length and mass.

we will arrive at a promising method which might one day be useful for generating energy-injecting VNHCs on arbitrary mechanical systems.

4.2 Dynamics of the Acrobot

Suppose we are given an acrobot as in Figure 4.1 modelling a gymnast hanging on a horizontal bar, where the "torso" has moment of inertia J_u and the "leg" has moment of inertia J_a (each with respect to their own center of mass). Let $q_u \in \mathbb{S}^1$ be the shoulder angle and $q_a \in \mathbb{S}^1$ be the hip angle, where only q_a is actuated. Collecting them together provides the configuration $q = (q_u, q_a) \in \mathbb{S}^1 \times \mathbb{S}^1$. The acrobot has inertia matrix D, potential function P (with respect to the horizontal bar), and input matrix B given as follows [21]:

$$D(q) = \begin{bmatrix} m_a l_u^2 + 2m_a \cos(q_a) l_u l_{c_a} + m_a l_{c_a}^2 + m_u l_{c_u}^2 + J_u + J_a & m_a l_{c_a}^2 + m_a l_u l_{c_a} \cos(q_a) + J_a \\ m_a l_{c_a}^2 + m_a l_u l_{c_a} \cos(q_a) + J_a & m_a l_{c_a}^2 + J_a \end{bmatrix}, \tag{4.1}$$

$$P(q) = g\left(m_a l_{c_a}(1 - \cos(q_u + q_a)) + (m_a l_u + m_u l_{c_u})(1 - \cos(q_u))\right), \tag{4.2}$$

$$B(q) = \begin{bmatrix} 0 \\ 1 \end{bmatrix}. \tag{4.3}$$

While this is the most general representation of an acrobot, the dynamics are unwieldy. To make rigorous analysis of these dynamics more tractable, we begin by assuming the acrobot is comprised of two massless rods of equal length l, with equal

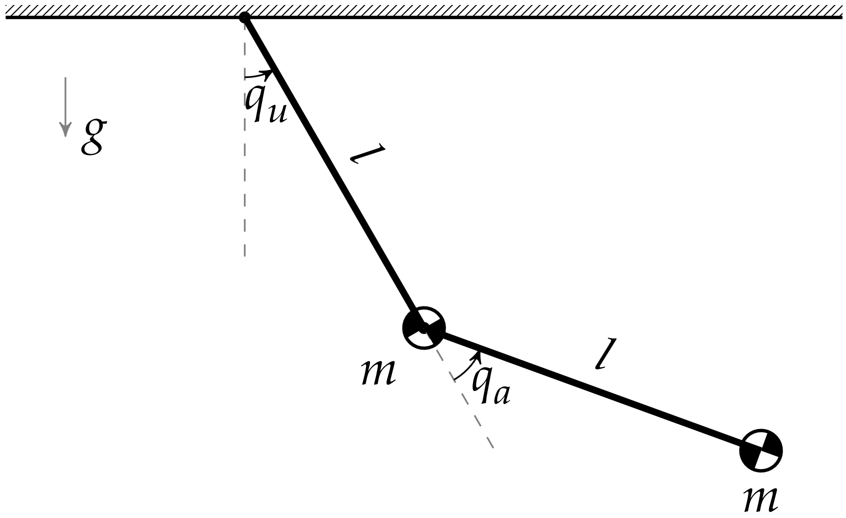

FIGURE 4.2: A simple acrobot has massless rods of equal length l and equal masses m at the tips.

point masses m at the tips. We call this a *simple* acrobot, which is displayed in Figure 4.2. We will also ignore any frictional forces at both the hip and shoulder joints. Finally, it is important to note that a real gymnast cannot swing their legs in full circles, though they are usually flexible enough to raise them parallel to the floor; for this reason, we assume that $q_a \in [-Q_a, Q_a]$ where $Q_a \in [\frac{\pi}{2}, \pi[$.

Since we are now working with a simple acrobot, we have $l_{c_u} = l_{c_a} = l_u = l_a = l$ and $m_u = m_a = m$. On top of this, the moments of inertia J_u and J_a of the rods vanish. Reducing (4.1)-4.2 yields the simplified inertia matrix D_s and potential function P_s, where

$$D_s(q) = \begin{bmatrix} ml^2\left(3 + 2\cos(q_a)\right) & ml^2\left(1 + \cos(q_a)\right) \\ ml^2\left(1 + \cos(q_a)\right) & ml^2 \end{bmatrix}, \tag{4.4}$$

$$P_s(q) = -mgl\left(2\cos(q_u) + \cos(q_u + q_a)\right). \tag{4.5}$$

Notation. For shorthand, we write $c_u := \cos(q_u)$, $c_a := \cos(q_a)$, and $c_{ua} := \cos(q_u + q_a)$. Likewise, $s_u := \sin(q_u)$, $s_a := \sin(q_a)$, and $s_{ua} := \sin(q_u + q_a)$.

Defining $M(q) := D_s(q)$ and $V(q) := P_s(q)$, we find the conjugate of momenta is

$p = (p_u, p_a) = M(q)\dot{q}$. The dynamics in (q, p) coordinates are given by

$$\mathscr{H}(q,p) = \frac{1}{2}p^\top M^{-1}(q)p - mgl\left(2c_u + c_{ua}\right), \tag{4.6}$$
$$\begin{cases} \dot{q} = M^{-1}(q)p \\ \dot{p}_u = -mgl\left(2s_u + s_{ua}\right) \\ \dot{p}_a = -\frac{1}{2}p^\top \nabla_{q_a} M^{-1}(q)p - mgls_{ua} + \tau, \end{cases}$$

where the inverse inertia matrix is

$$M^{-1}(q) = \frac{1}{ml^2\left(2 - c_a^2\right)}\begin{bmatrix} 1 & -\left(1 + c_a\right) \\ -\left(1 + c_a\right) & 3 + 2c_a \end{bmatrix}. \tag{4.7}$$

The control input is a force $\tau \in \mathbb{R}$ affecting only the dynamics of p_a, representing a torque acting on the hip joint. This means (q, p) are simply actuated coordinates inside the phase space $\mathcal{Q} \times \mathscr{P}$ where $\mathcal{Q} = \mathcal{Q}_u \times \mathcal{Q}_a := \mathbb{S}^1 \times \mathbb{S}^1$, and $\mathscr{P} = \mathscr{P}_u \times \mathscr{P}_a := \mathbb{R} \times \mathbb{R}$. This allows us to apply the theory of VNHCs from Chapter 2.

Let us define the VNHC $h(q, p) = q_a - f(q_u, p_u)$ of order 1, where $f \in C^2\left(\mathcal{Q}_u \times \mathscr{P}_u; \mathcal{Q}_a\right)$. Since $\nabla_{q_u} M^{-1}(q) = \mathbf{0}_{2\times 2}$, Theorem 2.10 tells us that this VNHC will be regular when the regularity matrix

$$dh_q M^{-1}(q)\begin{bmatrix} 0 \\ 1 \end{bmatrix},$$

is of full rank 1 on the constraint manifold Γ. Given that $dh_q = \begin{bmatrix} -\partial_{q_u} f & 1 \end{bmatrix}$, the regularity matrix evaluates to the scalar equation

$$\frac{(1 + c_a)\partial_{q_u} f(q_u, p_u) + (3 + 2c_a)}{ml^2(2 - c_a^2)}. \tag{4.8}$$

This is full rank if and only if the numerator does not change sign. The following proposition provides a sufficient condition for regularity.

Proposition 4.1. *A relation $h(q, p) = q_a - f(p_u) = 0$ for (4.6) with $f \in C^2\left(\mathscr{P}_u; \mathcal{Q}_a\right)$ is a regular VNHC of order 1.*

Proof. Since $\partial_{q_u} f = 0$, the regularity equation (4.8) is strictly positive for all values of q_a, and hence is full rank everywhere on the constraint manifold. By Theorem 2.10, h is a regular VNHC of order 1. □

Proposition 4.1 will be useful later, as we will not need to check regularity if we design a function of the unactuated momentum.

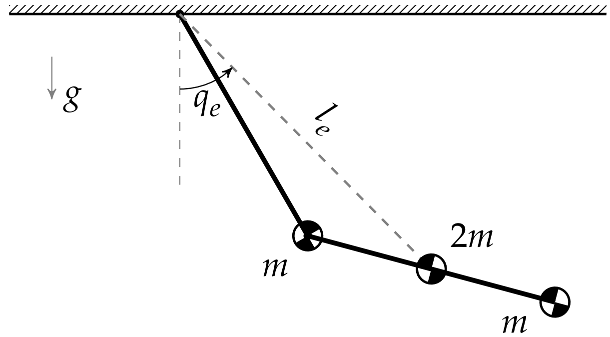

Figure 4.3: A simple acrobot modelled as a VLP with equivalent center of mass $2m$. The length of the VLP changes according to q_a.

The acrobot is noticeably more complex than the VLP, as the dynamics of (q_u, p_u) and (q_a, p_a) are coupled through $M^{-1}(q)$. Because of this, the constrained dynamics of an arbitrary VNHC may not be easy to write out. In the rest of this chapter, our goal is to design the function $f(q_u, p_u)$ based on the natural human motion of a gymnast, with one caveat: we must be able to prove the constrained dynamics will inject energy into the acrobot.

4.3 Previous Constraint Approaches

Let us examine some of the existing approaches to generating giant motion for the acrobot, since these may be viable candidates on which to base a VNHC.

One initial approach to controlling the acrobot is to model it as a variable-length pendulum by collapsing the two rods and masses into one equivalent center of mass (ECM), as in Figure 4.3. This seems a reasonable model reduction, since the length from the pivot to the ECM changes depending on the angle q_a of the leg. Indeed, Henmi et al. [18] use this approach to design a trajectory for the ECM, then determine which leg angles $q_a(t)$ are required to generate that trajectory. Following in their footsteps, we might consider using the results from Chapter 3 to find the leg angles that allow the ECM to gain energy. Then we could apply Theorem 3.2 to prove the acrobot is gaining energy.

Unfortunately, the VLP is not a true representation of the acrobot. The effective length of the ECM is

$$l_e(q_a) := l\sqrt{\frac{5}{4} + c_a},$$

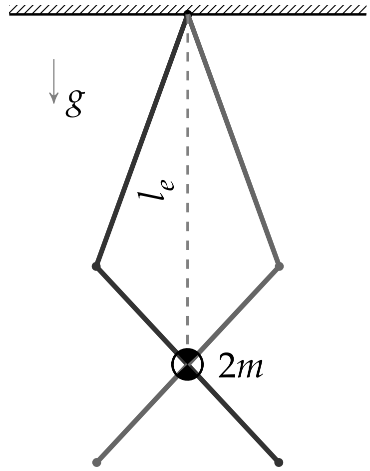

Figure 4.4: The equivalent center of mass of the acrobot generally has two configurations which correspond to the same effective length and angle. These configurations are symmetric about the line connecting the pivot to the ECM.

and its effective angle is

$$q_e := \arctan_2\left(s_u + \frac{1}{2}s_{ua}, -c_u - \frac{1}{2}c_{ua}\right).$$

There are two important notes to consider based on these equations. First, Figure 4.4 shows that for each pose of the VLP representation, there are two configurations of the acrobot which give the same effective length and angle. This means the acrobot and the VLP are not equivalent representations; designing a VNHC that injects energy using the ECM may not produce human-like leg motion on the acrobot.

Second, if we were to compute the conjugate of momenta p_{l_e} to l_e and p_e to q_e, we would see the torque input τ appearing in both of their dynamic equations. In the VLP model from Chapter 3, the control input only affects the dynamics of the length variable. If we want to design a VNHC for this system, we cannot use any of the results from Chapter 3 because the VLP models do not match.

Since we cannot apply the results of Chapter 3 to simplify the proof of energy injection, and the resulting ECM motion may not even produce realistic leg motion, this model reduction is ineffective for our purposes.

Let us turn next to the thesis of Wang [21], who designs a VHC to enforce a so-called "tap" motion with the purpose of injecting energy into the acrobot. First, he defines a compensator variable s which tracks $\dot{q}_u$, so that he can use the theory of VHCs with the extended configuration (q_u, q_a, s). He then finds $h_1, h_2 \in \mathbb{R}_{>0}$ to define the normalized radius ρ and normalized angle ξ in the (q_u, s)-plane. These normalized variables are given by

$$\rho := \sqrt{h_1 q_u^2 + h_2 s^2},$$
$$\xi := \arctan_2(h_2 s, h_1 q_u).$$

He then sets the VHC to be $h(q) = q_a - f_{\text{rad}}(\rho) f_{\text{ang}}(\xi)$ with the control parameters $\bar{q}_u$ and ρ_0, where

$$f_{\text{rad}}(\rho) := \tanh^2(\rho/\rho_0), \tag{4.9}$$

$$f_{\text{ang}}(\xi) := \begin{cases} 0 & -\pi < \xi \leq 0 \\ \bar{q}_u \exp\left(1 - \frac{1}{1-(\frac{4\xi}{\pi}-1)^2}\right) & 0 < \xi \leq \frac{\pi}{2} \\ 0 & \frac{\pi}{2} < \xi \leq \pi. \end{cases} \tag{4.10}$$

While this constraint shows promising experimental results and it accurately emulates true human motion, Wang does not provide analytical proof that the acrobot will gain energy. His lack of analysis is tied to the fact that the constrained dynamics are incredibly complicated. In fact, just showing the constraint is regular is a challenging task. While we could very easily convert his VHC into a VNHC by replacing s with p_u, we would run into the same problem. Since we want our constraint to *provably* inject energy, we must forgo this type of constraint in favour of something less complex.

4.4 The Acrobot Constraint

One may be tempted to design a constraint of the form $q_a = \bar{q}_a \sin(\theta)$ with $\theta := \arctan_2(p_u, q_u)$, since a similar approach was so effective for the VLP in Chapter 3. Unfortunately, this constraint is not regular, and it is difficult to find any VNHC of the form $q_a = f(\theta)$ where regularity can be proven easily. Instead, we will develop a constraint $h(q, p) = q_a - f(p_u)$ because these constraints are always regular (as per Proposition 4.1).

To design this constraint, let us begin (perhaps unexpectedly) by examining a person on a seated swing. The person extends their legs when the swing moves forwards, and retracts their legs when the swing moves backwards. As the swing gains speed, the person leans their body back while extending their legs. This allows them to bring their legs higher, shortening the distance from their center of mass to the pivot and adding more energy to the swing. When the swing moves backward, they sit up and

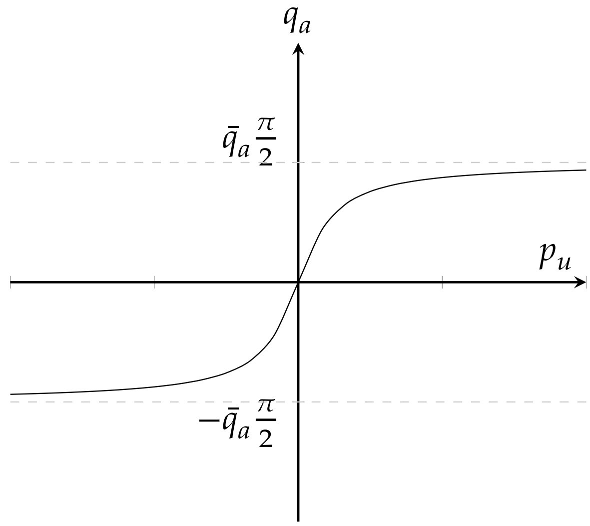

FIGURE 4.5: The acrobot constraint $q_a = \bar{q}_a \arctan(Ip_u)$.

fully retract their legs underneath them [8].

Now imagine the person's torso is affixed to the swing's rope so that they are always upright. Imagine further that the swing has no seat at all, allowing the person to extend their legs beneath them. This position is identical to that of a gymnast on a bar, which is why we can use leg motion from the seated swing to design a controller for the acrobot.

The acrobot's legs are rigid rods which cannot retract; so we emulate the person on a swing by pivoting the legs toward the direction of motion. To account for how a person leans back at higher speeds, the legs should pivot to an angle proportional to the swing's speed. Since the direction of motion is entirely determined by p_u, one such VNHC which emulates this process is $q_a = \bar{q}_a \arctan(Ip_u)$, displayed in Figure 4.5. Here, $\bar{q}_a \in]0, \frac{2Q_a}{\pi}]$ and $I \in \mathbb{R}_{>0}$ is a fixed control parameter.

This constraint does not perfectly recreate giant motion, during which the gymnast's legs are almost completely extended – it instead pivots the legs partially during rotations. However, the behaviour looks similar enough that the constraint should provide a decent foundation for injecting energy into the acrobot. It is for this reason that we choose our acrobot's constraint to be

$$h(q, p) = q_a - \bar{q}_a \arctan(Ip_u). \tag{4.11}$$

Let us now compute the constrained dynamics under (4.11). Note that $dh_q = \begin{bmatrix} 0 & 1 \end{bmatrix}$, while

$$dh_{p_u} = \frac{-\bar{q}_a I}{1 + I^2 p_u^2}.$$

Inserting these to (2.16), we get the solution for p_a on the constraint manifold:

$$p_a(q_u, p_u) = \frac{(1 + c_a)(1 + I^2 p_u^2)p_u - m^2 g l^3 \bar{q}_a I(2 - c_a^2)(2s_u + s_{ua})}{ml^2(3 + 2c_a)(1 + I^2 p_u^2)}.$$

The dynamics for p_u do not contain p_a, so they remain unchanged. The constrained dynamics for q_u are given by

$$\dot{q}_u = e_1^\top M^{-1}(q) \begin{bmatrix} p_u \\ p_a(q_u, p_u) \end{bmatrix},$$

which can be simplified into

$$\dot{q}_u = \frac{(1 + I^2 p_u^2)p_u + m^2 g l^3 \bar{q}_a I(2s_u + s_{ua})(1 + c_a)}{ml^2(1 + I^2 p_u^2)(3 + 2c_a)}.$$

Hence, the constrained dynamics for the acrobot under (4.11) are

$$\left.\begin{cases} \dot{q}_u &= \frac{(1+I^2p_u^2)p_u + m^2 g l^3 \bar{q}_a I(2s_u + s_{ua})(1+c_a)}{ml^2(1+I^2p_u^2)(3+2c_a)} \\ \dot{p}_u &= -mgl(2s_u + s_{ua}). \end{cases}\right|_{q_a = \bar{q}_a \arctan(Ip_u)} \tag{4.12}$$

These dynamics do not always gain energy – we need certain conditions on our control parameter I to guarantee this is true.

Theorem 4.2. *Consider the simple acrobot (4.6) constrained by the VNHC (4.11), whose constraint manifold is $\Gamma = \mathbb{S}^1 \times \mathbb{R}$. Let*

$$E(q_u, p_u) := \frac{p_u^2}{10ml^2} + 3(1 - \cos(q_u)),$$

be the energy of the simple pendulum obtained by setting $I = 0$.

1. *There always exists $I > 0$ small enough that (4.11) injects energy into the acrobot on the set*

$$\mathcal{O} := \left\{(q_u, p_u) \in \Gamma \mid E(q_u, p_u) < E(\pi, 0)\right\}.$$

If instead $I < 0$, the VNHC dissipates energy on $\mathcal{O}$.

2. *Define* $b : \mathbb{S}^1 \times \mathbb{R}_{>0} \to \mathbb{R}$ *by*

$$b(\beta, \rho_0) := \frac{5m^2gl^3\bar{q}_a\left(m^2gl^3\left(18s_\beta^2 + 30c_\beta(1-c_\beta)\right) - c_\beta\rho_0^2\right)}{|\rho_0|\sqrt{\rho_0^2 - 30m^2gl^3(1-c_\beta)}},$$

and fix $\bar{\rho} > \sqrt{60m^2gl^3}$. *Suppose* $\int_0^{2\pi} b(\sigma, \mu_0)d\sigma > 0$ *for all* $\rho_0 \in \left]\sqrt{60m^2gl^3}, \bar{\rho}\right[$. *Then there exists* $I > 0$ *small enough that* (4.11) *injects energy into the acrobot on*

$$\Omega := \left\{(q_u, p_u) \in \Gamma \mid E(q_u, p_u) < E(0, \bar{\rho})\right\}.$$

If instead $I < 0$, *the VNHC dissipates energy on* Ω.

The region $\mathcal{O}$ is the oscillation domain of the simple pendulum obtained by setting $q_a = 0$; Ω includes $\mathcal{O}$, alongside all rotations of this pendulum with momentum less than $\bar{\mu}$. Hence, the first result of Theorem 4.2 states that the acrobot will gain enough energy to begin performing giant motion; the second result guarantees can achieve giants with momentum $|p_u| < \bar{\mu}$.

Unfortunately, the energy-based proof used in Chapter 3 does not readily transfer to the acrobot – there is no obvious Lyapunov function for this constrained system. Proving Theorem 4.2 requires an intelligent change of coordinates and the use of perturbation theory from [22]. The full proof is given in Chapter 4.5, so we conclude this section with a high level sketch of the proof.

There is a suitable change of coordinates into a pseudo-radius $\mu \in \mathbb{R}_{>0}$ and pseudo-angle $\alpha \in \mathbb{S}^1$ on the (q_u, p_u)-plane. These coordinates have the property that $\dot{\alpha} > 0$ when I is small enough. Perturbation theory shows that (for possibly smaller I) the radius μ increases on average along α. Hence, orbits in the (q_u, p_u)-plane spiral away from the origin, which means the acrobot is gaining energy.

4.5 Proving the Acrobot Gains Energy

Proving Theorem 4.2 is not a simple task. In an effort to make the proof as clear as possible, we will break it down into the following segments:

1. Background on perturbation theory and averaging.

2. Perturbation analysis for oscillations.

3. Perturbation analysis for rotations.

(a) The simple pendulum with two masses.

(b) Level sets of the pendulum energy function. The red ellipse represents oscillations while the purple curve represents rotations.

Figure 4.6: Our constrained acrobot is a simple pendulum when $I = 0$.

When $I = 0$, the constrained acrobot behaves like a single pendulum with masses at a distance l and $2l$ from the pivot (Figure 4.6a) whose energy

$$E(q_u, p_u) = \frac{p_u^2}{10ml^2} + 3(1 - \cos(q_u)), \tag{4.13}$$

is conserved. Level sets of E are ellipses when $E(q_u, p_u) < E(\pi, 0)$, which we call "oscillations"; and they are open curves when $E(q_u, p_u) > E(\pi, 0)$, which we call "rotations". Examples of these can be seen in Figure 4.6b.

Using a method developed by Mohammadi et al. [4], we can find a change of coordinates $(q_u, p_u) \to (\alpha, \mu)$ with the following properties:

- The energy of oscillation in (α, μ) coordinates is uniquely defined by μ, which remains constant along oscillations of the simple pendulum.
- α is a pseudo-angle living in $\mathbb{S}^1$ which is always increasing.

Once we have these coordinates in hand, we can use perturbation theory to prove that μ increases on average for the acrobot when I is small enough. Likewise, we will find a second set of coordinates (β, ρ) where $\beta \in \mathbb{S}^1$ is always increasing, ρ is constant along rotations of the simple pendulum, and ρ increases for the acrobot when I is small enough. Putting these together, we will show the acrobot is gaining energy.

Background on Perturbation Theory

Nonlinear systems like the acrobot are difficult (or impossible) to solve analytically. Perturbation theory allows one to understand the behaviour of the nonlinear system by studying a simpler nominal system. Solutions of the nonlinear system can often be approximated by taking a Taylor expansion around this nominal system.

Khalil [22] considers a system of the form

$$\begin{cases} \dot{x} = f(t, x, \epsilon), \\ x(t_0) = \eta(\epsilon), \end{cases} \tag{4.14}$$

where $f : [t_0, t_1] \times D \times [-\epsilon_0, \epsilon_0] \to \mathbb{R}^n$ is sufficiently smooth. In the context of the acrobot, x is the set of coordinates which make our analysis convenient; ϵ is our control parameter I; the function f is the constrained dynamics in x-coordinates; and $\eta(\epsilon) \equiv \eta_0$ is a constant initial condition. To keep a notational reminder that we are applying perturbation theory to the acrobot, we will henceforth use I in place of ϵ.

Setting $I = 0$ we get the nominal system

$$\begin{cases} \dot{x}_0 = f(t, x, 0), \\ x_0(t_0) = \eta_0, \end{cases} \tag{4.15}$$

which we need to solve for the explicit solution $x_0(t, \eta_0)$ on $[t_0, t_1]$. One can use this to compute the solution $x_1(t, \eta_0)$ of

$$\begin{cases} \dot{x}_1 = \frac{\partial f}{\partial x}(t, x_0(t, \eta_0), 0)x_1 + \frac{\partial f}{\partial I}(t, x_0(t, \eta_0), 0), \\ x_1(t_0, \eta_0) = 0. \end{cases} \tag{4.16}$$

Finally, one can compute the first-order Taylor approximation $x(t, \eta_0) = x_0(t, \eta_0) + Ix_1(t, \eta_0) + R(t, I)$, where the remainder term $R(t, I)$ is $O(I^2)$, *i.e.*,

$$\lim_{I \to 0} \frac{R(t, I)}{I} = 0.$$

We now paraphrase Khalil's Theorem 10.1 [22] on the accuracy of perturbation analysis.

Theorem 4.3. *Suppose $f : [t_0, t_1] \times D \times [-I_0, I_0] \to \mathbb{R}^2$ is C^1, and that the nominal problem* (4.15) *has a unique solution $x_0(t, \eta_0) \in D$ on $[t_0, t_1]$. Then there exists $I^\star > 0$ such that for all I, $|I| < I^\star$, the solution $x(t, I, \eta_0)$ to* (4.14) *satisfies*

$$\|x(t, I, \eta_0) - \big(x_0(t, \eta_0) + Ix_1(t, \eta_0)\big)\| \le k|I^2|$$

for some $k > 0$.

Theorem 4.3 tells us that we can approximate the solution of the nonlinear system by the Taylor approximation $x(t, \eta_0) \approx x_0(t, \eta_0) + Ix_1(t, \eta_0)$. When I is small enough, solutions of the nonlinear system and the Taylor approximation are the same up to order I^2 along compact time intervals. Since we know that the acrobot behaves like a pendulum at $I = 0$, we can use this theory to prove energy injection properties on the acrobot by studying the simple pendulum.

FIGURE 4.7: The domain $\mathcal{O}$ where a pendulum oscillates. The pseudo-radius coordinate μ corresponds to the intersection of an orbit of oscillation with the q_u-axis.

Perturbation Analysis for Oscillations

As we have seen, the acrobot becomes a nominal pendulum that oscillates whenever the nominal energy (4.13) is less than $E(\pi, 0)$. Hence, the domain of oscillations for the nominal pendulum is given by

$$\mathcal{O} := \left\{(q_u, p_u) \in \Gamma \mid E(q_u, p_u) < E(\pi, 0)\right\},$$

where $\Gamma = \mathbb{S}^1 \times \mathbb{R}$ is the consraint manifold of the acrobot. We wish to find a transformation $T(q_u, p_u)$ on $\mathcal{O}$ into (α, μ)-coordinates where $\alpha \in \mathbb{S}^1$ is a pseudo-angle and $\mu > 0$ is a pseudo-radius. Since the energy of oscillation can be determined by the orbit's intersection with the q_u-axis (as in Figure 4.7) and $q_u \in]-\pi, \pi[$ on $\mathcal{O}$, we set $\mu \in]0, \pi[$. The transformation we want is therefore a diffeomorphism of the form

$$\begin{aligned} T : D\backslash\{(0,0)\} &\to \mathbb{S}^1 \times]0, \pi[, \\ (q_u, p_u) &\mapsto (\alpha, \mu). \end{aligned}$$

The energy level set corresponding to the intersection $(q_u, p_u) = (\mu, 0)$ is

$$\left\{(q_u, p_u) \in \Gamma \mid E(q_u, p_u) = 3mgl(1 - \cos(\mu))\right\},$$

which gives the relationship

$$p_u^2 = 30m^2gl^3(\cos(q_u) - \cos(\mu)). \tag{4.17}$$

On this level set, q_u ranges between $[-\mu, \mu]$ and can be uniquely parameterized by $q_u = \mu\cos(\alpha)$, where α is our desired pseudo-angle. Substituting this into (4.17), we get

$$p_u^2 = 30m^2gl^3(\cos(\mu\cos(\alpha)) - \cos(\mu)).$$

We want to find p_u as a function of (α, μ); noting that we can determine the sign of p_u from the sign of $\sin(\alpha)$, we get the (clockwise) parameterization

$$p_u = -\operatorname{sgn}(\sin(\alpha))\sqrt{30m^2gl^3\left(\cos(\mu c_\alpha) - c_\mu\right)}, \tag{4.18}$$

which is smooth for all $\mu \in]0, \pi[$.

We have thus found a transformation $T^{-1}(\alpha, \mu) = (q_u, p_u)$. We need the inverse of this map to get our diffeomorphism $T(q_u, p_u)$. Notice from (4.17) that

$$\cos(\mu) = -\frac{p_u^2}{30m^2gl^3} + \cos(q_u) =: C_\mu(q_u, p_u).$$

Since $\mu \in]0, \pi[$, we can uniquely express μ by

$$\mu = \arccos\left(C_\mu(q_u, p_u)\right). \tag{4.19}$$

Next we need to find α. Recall that

$$\cos(\alpha) = \frac{q_u}{\mu}, \tag{4.20}$$

which means

$$\sin(\alpha) = \pm\sqrt{1 - \frac{q_u^2}{\mu^2}}. \tag{4.21}$$

Using (4.18), we determine that $\operatorname{sgn}(\sin(\alpha)) = -\operatorname{sgn}\left(p_u\right)$. Putting together (4.20) and (4.21), we deduce that

$$\alpha = \arctan_2\left(-\operatorname{sgn}\left(p_u\right)\sqrt{1 - \frac{q_u^2}{\mu^2}}, \frac{q_u}{\mu}\right)\Bigg|_{\mu=\arccos(C_\mu(q_u,p_u))}. \tag{4.22}$$

Thus, (4.19) and (4.22) define our transformation into (α, μ)-coordinates on $\mathcal{O}$.

The acrobot's constrained dynamics in (α, μ)-coordinates can be computed by evaluating

$$\begin{aligned}
\dot{\mu} &= \frac{\partial \mu(q_u, p_u)}{\partial q}{}_u \dot{q}_u + \frac{\partial \mu(q_u, p_u)}{\partial p_u}\dot{p}_u\Bigg|_{(q_u,p_u)=T^{-1}(\mu,\alpha)}, \\
\dot{\alpha} &= \frac{\partial \alpha(q_u, p_u)}{\partial q_u}\dot{q}_u + \frac{\partial \alpha(q_u, p_u)}{\partial p_u}\dot{p}_u\Bigg|_{(q_u,p_u)=T^{-1}(\mu,\alpha)}.
\end{aligned}$$

with $(\dot{q}_u, \dot{p}_u)$ given by (4.12).

These dynamics are much too large to write out, so we simply denote them by

$$\dot{\mu} = f_\mu(\alpha, \mu, I), \tag{4.23}$$

$$\dot{\alpha} = f_\alpha(\alpha, \mu, I). \tag{4.24}$$

FIGURE 4.8: If the acrobot is initialized at $(q_u, p_u) = (\mu_0, 0)$, then either the orbit escapes $\mathcal{O}$ into the rotation zone (purple), or the orbit hits the other half of the q_u-axis with a higher (red), equal (black), or lower (blue) angle than when it started.

The dynamics of the nominal pendulum arise from evaluating f_μ and f_α at $I = 0$. MATLAB's symbolic toolbox evaluates the nominal dynamics as

$$\dot{\mu}_n = 0, \tag{4.25}$$

$$\dot{\alpha}_n = \sqrt{\frac{6g}{5l}}\sqrt{\frac{\cos(\mu_n \cos(\alpha_n)) - \cos(\mu_n)}{\mu_n^2 \sin(\alpha_n)^2}}. \tag{4.26}$$

Note that we write the nominal coordinates as (α_n, μ_n) to distinguish them from the acrobot's coordinates. One can confirm that $\dot{\alpha}_n > 0$ for every $\mu_n \in]0, \pi[$. This is expected of an oscillating single pendulum. By continuity of (4.23), $\dot{\alpha}$ remains positive on $\mathcal{O}$ for I small enough.

Suppose at time $t = 0$ we have initialized the acrobot at $(q_u, p_u) = (\mu_0, 0)$, which corresponds to $(\alpha, \mu) = (0, \mu_0)$. Since α is continuously increasing, we know that the orbit will do one of two things: it will either leave $\mathcal{O}$ so that the acrobot is now rotating, or it will remain in $\mathcal{O}$ and hit the q_u-axis at some point $(\alpha, \mu) = (\pi, m)$ (as illustrated in Figure 4.8). From there, the acrobot could escape $\mathcal{O}$ along the second half of the orbit or return to some point $(\alpha, \mu) = (0, \tilde{m})$. If $\tilde{m} < \mu_0$ then the acrobot has lost energy; if $\tilde{m} > \mu_0$ the acrobot has gained energy; and if $\tilde{m} = \mu_0$, the acrobot is on a closed orbit. Which situation occurs might depend entirely on the choice of μ_0.

Since $\dot{\alpha} > 0$, we could theoretically find some time scaling $t = \tau(\alpha)$ and use α as a new "time" variable. Setting $\hat{\mu}(\alpha) := \mu(\tau(\alpha))$ allows us to ignore the dynamics of α and study the evolution of μ as a function of α rather than as a function of t (assuming the acrobot does not leave $\mathcal{O}$). The dynamics of $\hat{\mu}$ are

$$\frac{d\hat{\mu}}{d\alpha} = \frac{d\mu}{dt}\frac{dt}{d\alpha}\bigg|_{t=\tau(\alpha)},$$

yielding the "time"-varying scalar ODE

$$\begin{cases} \frac{d\hat{\mu}}{d\alpha} = \frac{f_\mu(\tau(\alpha),\mu,I)}{f_\alpha(\tau(\alpha),\mu,I)} =: g(\alpha, \mu, I), \\ \hat{\mu}(0) = \mu_0. \end{cases} \tag{4.27}$$

with solution $\hat{\mu}(\alpha, \mu_0, I)$.

In the spirit of perturbation analysis, we expand the solution of (4.27) into

$$\hat{\mu}(\alpha, \mu_0, I) = \hat{\mu}_0(\alpha, \mu_0) + I\hat{\mu}_1(\alpha, \mu_0) + R(\alpha, \mu_0, I), \tag{4.28}$$

where $R(\alpha, \mu_0, I)$ is $O(I^2)$. From (4.15) we know that $\hat{\mu}_0$ is the solution to the nominal system

$$\begin{cases} \dot{\hat{\mu}}_0 = g(\alpha, \mu, 0), \\ \hat{\mu}_0(0) = \mu_0, \end{cases}$$

Since $g(\alpha, \mu, 0) = 0$ by (4.25)-(4.26), we find that $\hat{\mu}_0(\alpha, \mu_0) \equiv \mu_0$ for all α.

Likewise, (4.16) tells us that $\hat{\mu}_1$ is the solution to

$$\begin{cases} \dot{\hat{\mu}}_1 = a(\alpha, \mu_0)\hat{\mu}_1 + b(\alpha, \mu_0), \\ \hat{\mu}_1(0) = 0. \end{cases} \tag{4.29}$$

where

$$\begin{aligned} a(\alpha, \mu_0) &= \frac{\partial g}{\partial \hat{\mu}}(\alpha, \mu_0, 0), \\ b(\alpha, \mu_0) &= \frac{\partial g}{\partial I}(\alpha, \mu_0, 0). \end{aligned}$$

These are difficult to compute by hand, so we resort to MATLAB symbolic computation to reveal that

$$\begin{aligned} a(\alpha, \mu_0) &= 0, \\ b(\alpha, \mu_0) &= K\hat{b}(\alpha, \mu_0), \end{aligned}$$

where we define

$$\begin{aligned} K &:= \frac{\bar{q}_a\sqrt{30m^2gl^3}}{15}, \\ \hat{b}(\alpha, \mu_0) &:= \frac{\mu_0|\sin(\alpha)|\left(5c_{\mu_0}\cos(\mu_0 c_\alpha) - 8\cos(\mu_0 c_\alpha)^2 + 3\right)}{\sin(\mu_0)\sqrt{\cos(\mu_0 c_\alpha) - c_{\mu_0}}}. \end{aligned}$$

Hence, the solution to (4.29) is given by

$$\hat{\mu}_1(\alpha, \mu_0) = K\int_0^\alpha \hat{b}(\sigma, \mu_0)d\sigma.$$

Figure 4.9: The plot of $Q(\mu_0)$.

Notice that $\hat{b}(\alpha, \mu_0)$ is both even and π-periodic in α, so that the following properties hold:

$$\begin{aligned} \int_0^{N\pi} \hat{b}(\sigma, \mu_0) d\sigma &= N \int_0^{\pi} \hat{b}(\sigma, \mu_0) d\sigma \ \left(\forall N \in \mathbb{Z}_{>0}\right), \\ \int_{-\pi}^{0} \hat{b}(\sigma, \mu_0) d\sigma &= \int_0^{\pi} \hat{b}(\sigma, \mu_0) d\sigma. \end{aligned} \tag{4.30}$$

Suppose we initialize the acrobot at $(\alpha, \mu) = (0, \mu_0)$. After half an orbit, when $\alpha = \pi$, the acrobot will have a new pseudo-radius $m = \hat{\mu}(\pi, \mu_0)$. Hence, the change in pseudo-radius is $m - \mu_0 \approx I\hat{\mu}_1(\pi, \mu_0)$. After an additional half orbit, the acrobot lands on the positive q_u-axis with pseudo-radius $\tilde{m} \approx \mu_0 + I\hat{\mu}_1(2\pi, \mu_0)$. The properties outlined in (4.30) imply that $\hat{\mu}_1(2\pi, \mu_0) = 2\hat{\mu}_1(\pi, \mu_0)$. This means the change in pseudo-radius after one entire oscillation is $\tilde{m} - \mu_0 \approx 2I\hat{\mu}_1(\pi, \mu_0) \approx 2(m - \mu_0)$. Hence, if $\hat{\mu}_1(\pi, \cdot)$ is always positive, $\hat{\mu}$ must be increasing every half oscillation. This in turn would guarantee q_u is increasing, which means the acrobot will eventually reach a rotation.

To prove this intuitive argument rigorously, we define the Poincaré section $P_{\mathcal{O}}(\mu_0) := \hat{\mu}(\pi, \mu_0)$, which expands into

$$P_{\mathcal{O}}(\mu_0) = \mu_0 + I\hat{\mu}_1(\pi, \mu_0) + R(\pi, I).$$

Let us define

$$Q(\mu_0) := \int_0^{\pi} \hat{b}(\sigma, \mu_0) d\sigma,$$

so that $\hat{\mu}_1(\pi, \mu_0) = KQ(\mu_0)$. Note that K is a positive constant that takes into account the acrobot's mass and length, while $\hat{b}(\alpha, \mu)$ is adimensional; that is, it is the same for every possible choice of acrobot. Hence, $Q(\mu_0)$ is the same for every acrobot. If $Q(\mu_0)$ is strictly positive, then $\hat{\mu}_1(\pi, \mu_0)$ will be positive no matter the values of m, g, l, or $\bar{q}_a$.

We numerically compute $Q(\mu_0)$ for $\mu_0 \in [10^{-5}, \pi - 10^{-5}]$ in Figure 4.9. We see that $Q(\mu_0)$ is strictly positive and monotonically increasing, with an asymptote at $\mu_0 = \pi$. Simulations with smaller μ_0 vanish in MATLAB, so we believe that $Q(\mu_0)$ is in fact positive for all μ_0.

We conclude that, for all m, g, l, $\bar{q}_a$, and for small enough I, the Poincaré section $P_{\mathcal{O}}(\mu_0)$ is positive, monotonically increasing, and $\lim_{\mu_0 \to \pi} P_{\mathcal{O}}(\mu_0) = \infty$.

Suppose we initialize the acrobot at $(q_0, p_0) \in \mathscr{O}$. Since on $\mathscr{O}$ we have $\dot{\alpha} > 0$, the orbit of the acrobot in Γ spirals clockwise around the origin; if the spiral does not exit $\mathscr{O}$, it must intersect the q_u axis. Once it does, the Poincaré section $P_{\mathscr{O}}(\cdot)$ tells us the orbit must spiral away from the origin. This implies there cannot be any closed orbits in $\mathscr{O}$ and that the origin is a repeller.

Once the orbit reaches an intersection point $(\mu_0, 0)$ on the q_u-axis such that $P_{\mathscr{O}}(\mu_0) > \pi$, the orbit will no longer return to the q_u-axis. Instead, it will escape $\mathscr{O}$ entirely, which means it must escape any compact subset of $\mathscr{O}$ in finite time. We conclude that the acrobot is gaining energy on $\mathscr{O}$.

Setting $I < 0$, the Poincaré section $P_{\mathscr{O}}(\mu_0)$ is now decreasing. Hence, the orbit in $\mathscr{O}$ spirals towards the origin, which means the constraint is dissipating energy on $\mathscr{O}$.

□

Perturbation Analysis for Rotations

The rotation region for the nominal pendulum is the set

$$\mathscr{R} := \left\{(q_u, p_u) \in \Gamma \mid E(q_u, p_u) > E(\pi, 0)\right\}.$$

We wish to find a new set of coordinates (β, ρ) for the acrobot and perform a similar analysis to what we did for oscillations. In the oscillation region $\mathscr{O}$ we showed that the nominal pendulum's energy (and hence, its orbit) is uniquely determined by the intersection point μ with the q_u-axis; when the nominal pendulum is rotating, the energy is instead determined by the intersection ρ on the p_u-axis. Note that the boundary of $\mathscr{O}$ intersects the p_u axis when $p_u^2 = 60m^2gl^3$; hence, for a rotation we must have $\rho > \sqrt{60m^2gl^3}$ if the orbit has momentum $p_u > 0$ or $\rho < -\sqrt{60m^2gl^3}$ if the orbit has momentum $p_u < 0$. The energy level set associated with ρ is

$$\left\{(q_u, p_u) \in \Gamma \mid E(q_u, p_u) = \frac{\rho^2}{10ml^2}\right\},$$

which gives the relationship

$$\frac{p_u^2}{10ml^2} + 30mgl(1 - c_u) = \frac{\rho^2}{10ml^2}. \tag{4.31}$$

On this level set, q_u takes all values on $\mathbb{S}^1$, so our angle of rotation is uniquely parameterized by $\beta = q_u$. Since ρ does not change sign along the rotation, we have the smooth relationship

$$q_u = \beta, \tag{4.32}$$

$$p_u = \operatorname{sgn}(\rho)\sqrt{\rho^2 - 30m^2gl^3\left(1 - c_\beta\right)}. \tag{4.33}$$

Inverting this relationship gives our (smooth) transformation

$$T : \mathbb{S}^1 \times \mathbb{R} \to \mathbb{S}^1 \times]-\infty, -60m^2gl^3[\, \cup\,]60m^2gl^3, \infty[,$$

where $T(q_u, p_u) = (\beta, \rho)$ is defined by

$$\beta = q_u, \tag{4.34}$$

$$\rho = \operatorname{sgn}(p_u)\sqrt{p_u^2 + 30m^2gl^3\left(1 - c_u\right)}. \tag{4.35}$$

Computing the acrobot's constrained dynamics in (β, ρ)-coordinates and setting $I = 0$ yields the dynamics of the nominal pendulum. MATLAB evaluates those dynamics as

$$\dot{\rho}_n = 0, \tag{4.36}$$

$$\dot{\beta}_n = \operatorname{sgn}(\rho)\frac{\sqrt{\rho^2 - 30m^2gl^3(1 - c_\beta)}}{5ml^2}. \tag{4.37}$$

As expected, $\dot{\beta}_n$ does not change sign on $\mathscr{R}$ because a rotating pendulum does not change direction: if $\rho_n > 0$, the orbit traces a curve going from $\beta_n = -\pi$ to $\beta_n = \pi$; if $\rho_n < 0$ the curve goes in the reverse direction. By continuity of the acrobot's constrained dynamics $(\dot{\beta}, \dot{\rho})$, we must also have $\operatorname{sgn}(\dot{\beta}) = \operatorname{sgn}(\rho_0)$ for small enough I. Hence, we can use β as a new "time" variable on $\mathscr{R}$ by performing a time transformation $t = \tau(\beta)$. This produces the time-scaled system $\hat{\rho}(\beta) = \rho(\tau(\beta))$ with dynamics

$$\begin{cases} \dot{\hat{\rho}} = \frac{\dot{\rho}}{\dot{\beta}}, \\ \hat{\rho}(0) = \rho_0. \end{cases}$$

For a perturbation approach, be expand the solution of these dynamics into

$$\hat{\rho}(\beta, \rho_0, I) = \hat{\rho}_0(\beta, \rho_0) + I\hat{\rho}_1(\beta, \rho_0) + R(\beta, \rho_0, I), \tag{4.38}$$

where $R(\beta, \rho_0, I)$ is $O(I^2)$.

From (4.15) we know $\hat{\rho}_0$ is the solution to the nominal system

$$\begin{cases} \dot{\hat{\rho}}_0 = 0, \\ \hat{\mu}_0(0) = \rho_0, \end{cases}$$

which means $\hat{\mu}_0(\beta, \rho_0) \equiv \rho_0$ for all β. Likewise, (4.16) gives us the following dynamics for $\hat{\rho}_1$:

$$\begin{cases} \dot{\hat{\rho}}_1 = \frac{5m^2gl^3\bar{q}_a\left(m^2gl^3\left(18s_\beta^2+30c_\beta(1-c_\beta)\right)-c_\beta\rho_0^2\right)}{|\rho_0|\sqrt{\rho_0^2-30m^2gl^3(1-c_\beta)}} =: b(\beta, \rho_0), \\ \hat{\rho}_1(0) = 0. \end{cases} \tag{4.39}$$

The solution to (4.39) is given by

$$\hat{\rho}_1(\beta, \rho_0) = \int_0^\beta b(\sigma, \rho_0) d\sigma.$$

Supposing we initialize the acrobot at $(\beta, \rho) = (0, \rho_0)$, then one full rotation amounts to β traversing 2πrad in a clockwise direction (*i.e.*β going from 0 to $\operatorname{sgn}(\rho_0) 2\pi$). We define a Poincaré section as the point reached on the p_u axis after every rotation:

$$P_{\mathscr{R}}(\rho_0) = \rho_0 + I\hat{\rho}_1(\operatorname{sgn}(\rho_0) 2\pi, \rho_0) + R(2\pi, I).$$

If $|P_{\mathscr{R}}(\rho_0)| > |\rho_0|$, then the rotation has driven the orbit further from the origin. In other words, $|p_u|$ has increased across the rotation. If this is true for any ρ_0, the acrobot is gaining momentum, which in turn means it is gaining energy.

The function $b(\beta, \rho_0)$ is even in both its inputs, and is 2π-periodic in β. Hence, we have

$$\begin{aligned} \hat{\rho}_1(\operatorname{sgn}(\rho_0) 2\pi, \rho_0) &= \int_0^{\operatorname{sgn}(\rho_0)2\pi} b(\sigma, \rho_0) d\sigma, \\ &= \operatorname{sgn}(\rho_0) \int_0^{2\pi} b(\sigma, \rho_0) d\sigma, \\ &= \operatorname{sgn}(\rho_0) \hat{\rho}_1(2\pi, \rho_0). \end{aligned}$$

Furthermore, $\hat{\rho}_1(2\pi, \rho_0) = \hat{\rho}_1(2\pi, |\rho_0|)$. This implies that

$$|P_{\mathscr{R}}(\rho_0)| = \left|\operatorname{sgn}(\rho_0)\left(|\rho_0| + I\hat{\rho}_1(2\pi, |\rho_0|)\right)\right| = P_{\mathscr{R}}(|\rho_0|).$$

Figure 4.10: The set W of points which have pseudo-radius $|\rho| \in]\sqrt{60m^2gl^3}, \bar{\rho}[$. The inner boundary of W is $(q_u, p_u) = (\pi, 0)$, which is also the boundary of the oscillation domain *mathcalO*.

Hence, if $P_{\mathscr{R}}(|\rho_0|) > |\rho_0|$ (or equivalently if $\hat{\rho}_1(2\pi, |\rho_0|) > 0$) the phase $(q_u(t), p_u(t))$ initialized at $(0, \rho_0)$ will intersect the p_u axis at a point $p > \rho_0$. If we could guarantee that $\hat{\rho}_1(2\pi, \rho_0) > 0$ for all $\rho_0 > \sqrt{60m^2gl^3}$, then the acrobot would be spiraling away from the origin on $\mathscr{R}$.

Unfortunately, we cannot adimensionalize $b(\beta, \rho_0)$ like we did for oscillations. Using the assumption , we have that $\hat{\rho}_1(2\pi, \rho_0) > 0$ for all $\rho_0 \in]\sqrt{60m^2gl^3}, \rho_0[$. We conclude that, for small enough I, the Poincaré section $P_{\mathscr{R}}(\rho_0)$ is monotonically increasing when $0 < \rho_0 < \bar{\rho}$ and monotonically decreasing when $-\bar{\rho} < \rho_0 < 0$.

Proving Energy Gain

We will prove the acrobot gains energy on the set

$$\Omega := \left\{(q_u, p_u) \in \Gamma \mid E(q_u, p_u) < E(0, \bar{\rho})\right\}.$$

Define the set of points in $\mathscr{R}$ which have pseudo-radius in U by

$$W := \left\{(q_u, p_u) \in \Gamma \mid |\rho(q_u, p_u)| \in U\right\},$$

as in Figure 4.10. Monotonicity of $P(\rho_0)$ means there are no closed orbits of (q_u, p_u) on W. Furthermore, $|p_u|$ is increasing every time the orbit hits the p_u-axis.

We conclude that $|\rho(q_u, p_u)|$ will eventually reach $\bar{\rho}$. We cannot claim this fits the definition of energy injection (since $(0, 0) \notin W$), but we can still say that (q_u, p_u) will eventually depart W through the outer boundary in finite time. The acrobot is thereby gaining energy in the literal sense that its momentum is increasing on W.

If we set $I < 0$, we have $P(|\rho_0|) < |\rho_0|$. Hence, $|p_u|$ is decreasing every time the orbit hits the p_u-axis, so the acrobot will eventually depart W through the inner boundary. The acrobot is losing momentum, and therefore it is losing energy on W.

A hybrid supervisor that flips the sign of I based on the current value of μ will stabilize any energy level of oscillation. As was the case in the VLP, this supervisor should implement some kind of hysteresis to avoid infinite switching.

4.6 Experimental Results

Chapter 5

Conclusion

5.1 Limitations of this Work

5.2 Future Research

Appendix A

Bounding the Acrobot Control Parameter

Bibliography

[1] F. Udwadia, "Constrained motion of hamiltonian systems," *Nonlinear Dynamics*, vol. 84, no. 3, pp. 1135 – 1145, December 2015.

[2] K. Ono, K. Yamamoto, and A. Imadu, "Control of giant swing motion of a two-link horizontal bar gymnastic robot," *Advanced Robotics*, vol. 15, no. 4, pp. 449 – 465, 2001.

[3] X. Zhang, H. Cheng, Y. Zhao, and B. Gao, "The dynamical servo control problem for the acrobot based on virtual constraints approach," in *The 2009 IEEE/RSJ International Conference on Intelligent Robots and Systems*. St. Louis, USA: IEEE, October 2009.

[4] A. Mohammadi, M. Maggiore, and L. Consolini, "Dynamic virtual holonomic constraints for stabilization of closed orbits in underactuated mechanical systems," *Automatica*, vol. 94, pp. 112 – 124, August 2018.

[5] E. Papadopoulos and G. Papadopoulos, "A novel energy pumping strategy for robotic swinging," in *2009 17th Mediterranean Conference on Control and Automation*. Thessaloniki, Greece: IEEE, June 2009.

[6] A. J. V. der Schaft, "On the hamiltonian formulation of nonholonomic mechanical systems," *Reports on Mathematical Physics*, vol. 34, no. 2, pp. 225 – 233, 1994.

[7] O. E. Fernandez, "The hamiltonization of nonholonomic systems and its applications," Ph.D. dissertation, University of Michigan, 2009.

[8] S. Wirkus, R. Rand, and A. Ruina, "How to pump a swing," *The College Mathematics Journal*, vol. 29, no. 4, pp. 266 – 275, 1998.

[9] J. Horn, A. Mohammadi, K. Hamed, and R. Gregg, "Hybrid zero dynamics of bipedal robots under nonholonomic virtual constraints," *IEEE Control Systems Letters*, vol. 3, no. 2, pp. 386 – 391, April 2019.

[10] S. C. Anco and G. Bluman, "Integrating factors and first integrals for ordinary differential equations," *European Journal of Applied Mathematics*, vol. 9, pp. 245 – 259, 1998.

[11] A. Mohammadi, M. Maggiore, and L. Consolini, "On the lagrangian structure of reduced dynamics under virtual holonomic constraints," *ESAIM: Control, Optimization and Calculus of Variations*, vol. 23, no. 3, pp. 913 – 935, June 2017.

[12] M. S. Branicky, "Multiple lyapunov functions and other analysis tools for switched and hybrid systems," *IEEE Transactions on Automatic Control*, vol. 43, no. 4, pp. 475 – 482, April 1998.

[13] J. Lu and L. J. Brown, "A multiple lyapunov functions approach for stability of switched systems," in *2010 American Control Conference*. Baltimore, USA: IEEE, July 2010.

[14] A. M. Bloch, J. E. Marsden, and D. V. Zenkov, "Nonholonomic dynamics," *Notices of the AMS*, vol. 52, no. 3, pp. 320 – 329, March 2005.

[15] V. Sevrez, E. Berton, G. Rao, and R. J. Bootsma, "Regulation of pendulum length as a control mechanism in performing the backward giant circle in gymnastics," *Human Movement Science*, vol. 28, no. 2, pp. 250 – 262, March 2009.

[16] B. Piccoli and J. Kulkarni, "Pumping a swing by standing and squatting: Do children pump time-optimally?" *IEEE Control Systems Magazine*, vol. 25, no. 4, pp. 48 – 56, August 2005.

[17] A. D. Mahindrakar and R. N. Banavar, "A swing-up of the acrobot based on a simple pendulum strategy," *International Journal of Control*, vol. 78, no. 6, pp. 424 – 429, 2005.

[18] T. Henmi, M. Chujo, Y. Ohta, and M. Deng, "Reproduction of swing-up and giant swing motion of acrobot based on a technique of the horizontal bar gymnast," in *Proceedings of the 11th World Congress on Intelligent Control and Automation*. Shenyang, China: IEEE, June 2014.

[19] M. Maggiore and L. Consolini, "Virtual holonomic constraints for euler-lagrange systems," *IEEE Transactions on Automatic Control*, vol. 58, no. 4, pp. 1001 – 1008, April 2013.

[20] X. Xin and Y. Liu, "Trajectory tracking control of variable length pendulum by partial energy shaping," *Communications in Nonlinear Science and Numerical Simulations*, vol. 19, no. 5, pp. 1544 – 1556, May 2014.

[21] X. Wang, "Motion control of a gymnastics robot using virtual holonomic constraints," Master's thesis, University of Toronto, 2016.

[22] H. K. Khalil, *Nonlinear Systems*, 3rd ed. Upper Saddle River, NJ 07485: Prentice Hall, 2002.

[23] D. T. Greenwood, *Principles of Dynamics*, 2nd ed. Englewood Cliffs, NJ: Prentice Hall, 1987.

[24] L. D. Landau and E. M. Lifschitz, *Mechanics*, 3rd ed. Butterworth-Heinemann, January 1982.

[25] J. A. Acosta, R. ortega, A. Astolfi, and A. Mahindrakar, "Interconnection and damping assignment passivity-based control of mechanical systems with underactuation degree one," *IEEE Transactions on Automatic Control*, vol. 50, no. 12, pp. 1936 – 1955, December 2005.

[26] A. Mahindrakar, A. Astolfi, R. Ortega, and G. Viola, "Further constructive results on interconnection and damping assignment control of mechanical systems: The acrobot example," in *Proceedings of the 2006 American Control Conference*. Minneapolis, Minnesota, USA: American Control Conference, June 2006.

[27] J. Grizzle, C. Chevallereau, R. Sinnet, and A. Ames, "Models, feedback control, and open problems of 3d bipedal robotic walking," *Automatica*, vol. 50, no. 8, pp. 1955 – 1988, August 2014.

[28] F. Plestan, J. Grizzle, E. R. Westervelt, and G. Abba, "Stable walking of a 7-dof biped robot," *IEEE Transactions on Robotics and Automation*, vol. 19, no. 4, pp. 653–668, August 2003.

[29] A. Mohammadi, E. Rezapour, M. Maggiore, and K. Y. Pettersen, "Maneuvering control of planar snake robots using virtual holonomic constraints," *IEEE Transactions on Control Systems Technology*, vol. 24, no. 3, pp. 884 – 899, May 2015.

[30] L. Consolini and M. Maggiore, "Control of a bicycle using virtual holonomic constraints," *Automatica*, vol. 49, no. 9, pp. 2831–2839, September 2013.

[31] S. Westerberg, U. Mettin, A. S. Shiriaev, L. B. Freidovich, and Y. Orlov, "Motion planning and control of a simplified helicopter model based on virtual holonomic constraints," in *2009 International Conference on Advanced Robotics*. Munich, Germany: IEEE, June 2009, pp. 1–6.

[32] T. Takubo, H. Arai, and K. Tanie, "Virtual nonholonomic constraint for human-robot cooperation in 3-d space," in *2000 IEEE/RSJ International Conference on Intelligent Robots and Systems*. Takamatsu, Japan: IEEE, October 2000.

[33] S. Shibata and T. Murakami, "Psd based virtual nonholonomic constraint for human interaction of redundant manipulator," in *Proceedings of the 2004 IEEE International Conference on Control Applications*. Taipei,Taiwan: IEEE, September 2004.

[34] J. D. Castro-Díaz, P. Sánchez-Sánchez, A. Gutiérrez-Giles, M. Arteaga-Pérez, and J. Pliego-Jiménez, "Experimental results for haptic interaction with virtual holonomic and nonholonomic constraints," *IEEE Access*, vol. 8, pp. 120 959 – 120 973, July 2020.

[35] S. Vozar, Z. Chen, P. Kazanzides, and L. L. Whitcomb, "Preliminary study of virtual nonholonomic constraints for time-delayed teleoperation," in *2015 IEEE/RSJ International Conference on Intelligent Robots and Systems*. Hamburg, Germany: IEEE, October 2015.

[36] B. Griffin and J. Grizzle, "Nonholonomic virtual constraints for dynamic walking," in *2015 54th IEEE Conference on Decision and Control*. Osaka, Japan: IEEE, December 2015.

[37] J. C. Horn, A. Mohammadi, K. A. Hamed, and R. D. Gregg, "Nonholonomic virtual constraint design for variable-incline bipedal robotic walking," *IEEE Robotics and Automation Letters*, vol. 5, pp. 3691 – 3698, February 2020.

[38] W. K. Chan, Y. Gu, and B. Yao, "Optimization of output functions with nonholonomic virtual constraints in underactauted bipedal walking control," in *2018 Annual American Control Conference*. Milwaukee, USA: IEEE, June 2018.

[39] A. O. Belyakov, A. P. Seyranian, and A. Luongo, "Dynamics of the pendulum with periodically varying length," *Physica D*, vol. 238, pp. 1589 – 1597, August 2009.

[40] C. Li, Z. Zhang, X. Liu, and Z. Shen, "An improved principle of rapid oscillation suppression of a pendulum by a controllable moving mass: Theory and simulation," *Shock and Vibration*, vol. 2019, April 2019.

[41] L. Wang, W. Shi, and Y. Zhou, "Study on self-adjustable variable pendulum tuned mass damper," *The structural design of tall and special buildings*, vol. 28, January 2019.

[42] A. M. Lyapunov, "The general problem of stability of motion (in russian)," Ph.D. dissertation, University of Kharkhov, Kharkhov, Russia, 1892.

[43] J. Hauser and R. Murray, "Nonlinear controllers for non-integrable systems: the acrobot example," in *1990 American Control Conference*. San Diego, USA: IEEE, May 1990.

[44] E. Westervelt, "Toward a coherent framework for the control of planar biped locomotion," Ph.D. dissertation, University of Michigan, Michigan, USA, 2003.

[45] M. W. Spong, "The swing up control problem for the acrobot," *IEEE Control Systems Magazine*, vol. 15, pp. 49–55, February 1995.

[46] X. Xin and M. Kaneda, "The swing up control for the acrobot based on energy control approach," in *Proceedings of the 41st IEEE Conference on Decision and Control*. Las Vegas, USA: IEEE, March 2003.

[47] T. Henmi, M. Akiyama, and T. Yamamoto, "Motion control of underactuated linkage robot based on gymnastic skill," *Electrical Engineering in Japan*, vol. 206, pp. 42–50, January 2009.

[48] P. E. Pidcoe, "The biomechanics principles behind training giant swings," Online, Virginia Commonwealth University, Richmond, VA, USA, August 2005, accessed 11 September 2020. https://usagym.org/pages/home/publications/technique/2005/8/giant.pdf.

[49] G. Golub and W. Kahan, "Calculating the singular values and pseudo-inverse of a matrix," *Journal of the Society for Industrial and Applied Mathematics: Series B, Numerical Analysis*, vol. 2, no. 2, pp. 204–224, 1965.

[50] E. A. Barbashin and N. N. Krasovskii, "On the stability of motion as a whole (in russian)," *Doklady Akademii Nauk SSSR*, vol. 86, pp. 453–456, 1952.

[51] R. D. Schafer, *An Introduction to Non-Associative Algebras*. New York: Dover Publications, 1996.

[52] I. Bendixson, "Sur les courbes définies par les équations différentielles," *Acta Math*, vol. 24, pp. 1–88, 1901.

[53] L. Perko, *Differential equations and dynamical systems*, 3rd ed. New York, USA: Springer, 2013, vol. 7.